Journal of Volcanology and Geothermal Research 266 (2013) 50–68

Contents lists available at ScienceDirect

Journal of Volcanology and Geothermal Research

journal homepage: www.elsevier.com/locate/jvolgeores

Geochemical constraints on the relationship between the Miocene–Pliocene volcanism and tectonics in the Palaoco and Fortunoso volcanic fields, Mendoza Region, Argentina: New insights from $^{40}Ar/^{39}Ar$ dating, Sr–Nd–Pb isotopes and trace elements

Charlotte T. Dyhr [a,*], Paul M. Holm [a], Eduardo J. Llambías [b]

[a] Department of Geography and Geology, University of Copenhagen, Oster Voldgade 10, DK-1350 Copenhagen, Denmark
[b] Universidad Nacional de La Plata, Calle 1#644, La Plata, Argentina

ARTICLE INFO

Article history:
Received 13 January 2013
Accepted 12 August 2013
Available online 29 September 2013

Keywords:
Back-arc volcanism
Geochemistry
Radiogenic isotopes
Payenia
$^{40}Ar/^{39}Ar$ dating
Flat slab

ABSTRACT

New $^{40}Ar/^{39}Ar$ analyses constrain the formation of the volcanic succession of Sierra de Palaoco in the present back-arc of the Andean Southern Volcanic Zone (SVZ), near 36°S, to the Late Miocene and assigns them to the Huincán II Formation. The composition of major and trace elements, Sr, Nd and Pb isotopes of the Palaoco and nearby Río Grande rocks require a strong arc-like component in the mantle that is absent or weak in both Early Miocene (Fortunoso Group) and Pleistocene alkaline lavas (Llancanelo Group) erupted in the same area. We evaluate the relative roles of varying mantle source compositions and crustal contamination in the generation of geochemically very different lavas from the Palaoco, Fortunoso and Río Grande volcanic fields, north of the Payún Matrú Volcano. The source for the Early Miocene Fortunoso(I) basalts was a OIB-type mantle devoid of subduction zone input. This type of OIB-like volcanic activity terminated due to a change from an extensional to a compressional tectonic regime. Towards the end of the Miocene renewed alkaline volcanism at Fortunoso (II) display a transition to arc-type incompatible element enrichment. Shortly after the calc-alkaline Palaoco volcanism started with a very strong geochemical arc-signature including Ba/La ≈ 60 and La/Nb = 2–3. After a quiesence of 1 Ma the major part of the voluminous Late Palaoco basalts were erupted around 7.5 Ma over a few hundred ka. These are less enriched in Ba and Sr and have compositions like many Holocene rocks of the Southern Volcanic Zone. Isotopically the Fortunoso I and Palaoco rocks are distinct. Regional volcanism of the Charilehue, Huincán I and II mostly has a moderate arc-type enrichment indicating incipient arc developments. However, Palaoco and La Brea at (c. 35°S) show full geochemical arc-signature, and we infer that a frontal arc was established. The subsequent development in the Palaoco-Río Grande area encompasses renewed late Pliocene calc-alkaline low volume volcanic eruptions (Río Grande group) succeeded in the Late Pleistocene by alkaline OIB-type eruptions (Llancanelo group). In the light of the course of volcanism to the east, in the Nevado area, where late Miocene–Pliocene calc-alkaline volcanism was followed by Late Pliocene–Pleistocene alkaline volcanism. We propose a scenario where the Nazca plate developed an eastwards widening flat slab from which the east dipping slab before the Late Pliocene translated from Palaoco to Nevado and subsequently retreated passing Río Grande in the Late Pliocene. Alkaline back-arc volcanism was active east of the arc-volcanism and expanded westwards during the Late Pliocene and Pleistocene.

1. Introduction

The purpose of this study is to characterize the volcanological, petrological and geochemical features of the Palaoco, Fortunoso and Río Grande volcanic rocks (Fig. 1) and to test a suggested model for transient Miocene to Pliocene shallow subduction of the Nazca plate beneath a region further to the south in Mendoza (Kay et al., 2004; Kay and Copeland, 2006; Kay et al., 2006b). The evolution of Sierra de Palaoco is evaluated in the light of new fieldwork, whole-rock major- and trace element analyses, new Sr, Nd and Pb isotopic data and radiometric dating. The Palaoco rocks are shown to be extremely arc-like and chemical contrasts with Early Miocene intraplate-like Fortunoso Group lavas and post-Miocene intraplate-like Llancanelo basalts are explored. The Palaoco and Fortunoso volcanic areas are volumetrically important among Miocene Payenia occurrences and have previously been little geochemically investigated (Nullo et al., 2002; and references therein).

Following the nomenclature of Hernando et al. (2012) volcanism occurring in the back-arc between 35°S and 38°S (Miocene–Holocene) is referred to as the Payenia Province or simply Payenia. Payenia covers approximately 15,900 km^2 (Bermúdez et al., 1993; Folguera et al.,

* Corresponding author. Tel.: +45 3532 2467.
E-mail addresses: ctd@geo.ku.dk (C.T. Dyhr), paulmh@geo.ku.dk (P.M. Holm), llambias@cig.museo.unlp.edu.ar (E.J. Llambías).

0377-0273/$ – see front matter © 2013 Elsevier B.V. All rights reserved.
http://dx.doi.org/10.1016/j.jvolgeores.2013.08.005

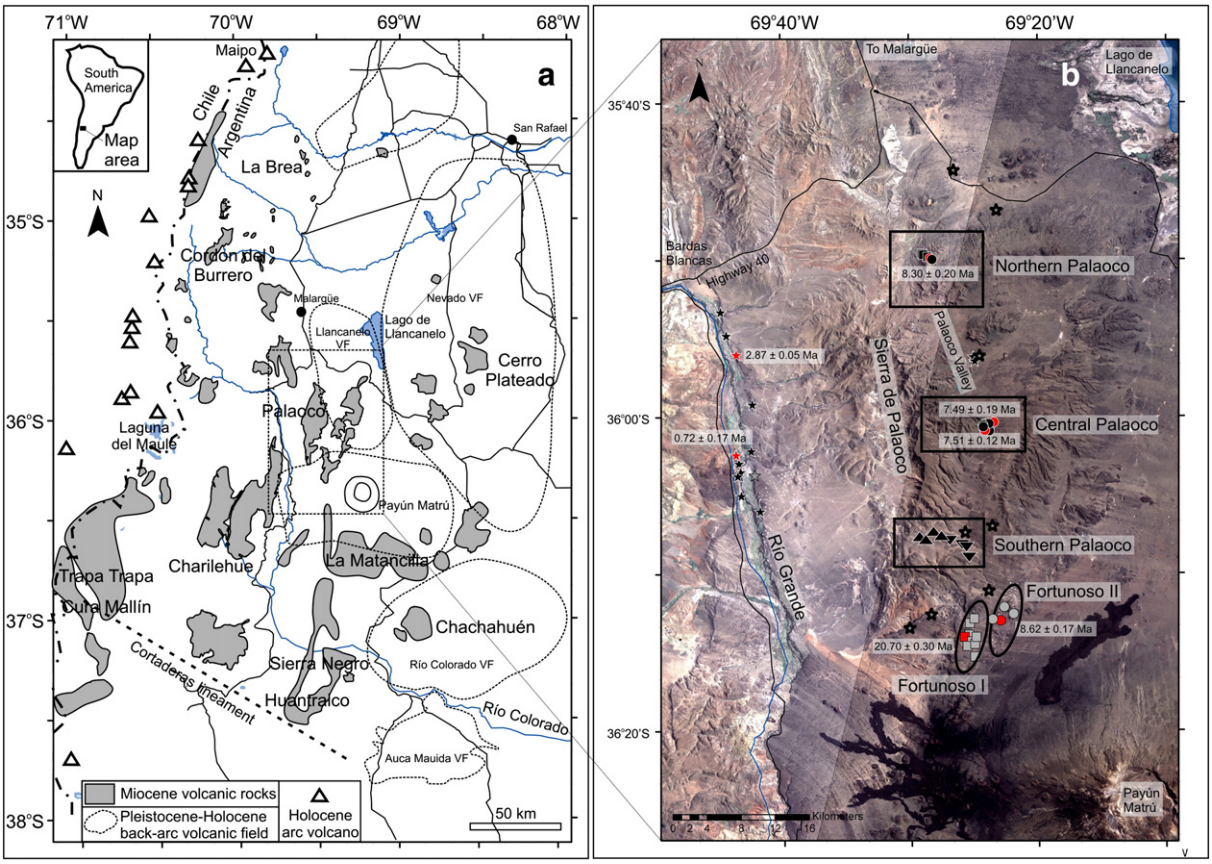

Fig. 1. a) Generalized map of selected volcanic areas of southern Mendoza and northern Neuquén based on Nullo et al. (2002), Kay and Copeland (2006), Ramos and Kay (2006), Litvak et al. (2008), Sruoga et al. (2008), Gudnason et al. (2012), Spagnuolo et al. (2012) and b) satellite image showing the Palaoco, Fortunoso, Río Grande and Llancanelo and all analyzed samples. Symbols are as in Fig. 3 and red symbols denote dated samples.

2009; Llambías et al., 2010). Bermúdez et al. (1993) divides the province into two distinct volcanic fields; the Llancanelo Volcanic Field in the north (10,700 km^2) and the Payún Matrú Volcanic Field in the south (5200 km^2) and Gudnason et al. (2012) subdivided Payenia into 5 volcanic fields and a retro-arc area (Fig. 1). More than 800 monogenetic cones are scattered throughout the province. Polygenetic cones in the present back-arc between 35°S and 38°S are also common, e.g. Chachahuén (Late Miocene), Nevado (Pliocene), Auca Mahuida (Pleistocene) and Payún Matrú (Late Pleistocene-Holocene) (Inbar and Risso, 2001; Llambías et al., 2010). The volcanism of Payenia may be divided into three distinct episodes differentiated by age, composition and tectonic affinity. The first episode occurred during the Early Miocene and is represented by La Matancilla (Kay and Copeland, 2006; Dyhr et al., 2013) and the here presented Fortunoso Group lavas of alkaline character. The second episode occurred during the Middle–Late Miocene and is represented by Palaoco, Chachahuén (Kay et al., 2006b), Huincán (Nullo et al., 2002; Sruoga et al., 2008; Spagnuolo et al., 2012) and Plateado/Pelado volcanoes (Litvak et al., 2008, 2009) all with arc-like geochemical affinities. The third episode occurred in the Late Pliocene–Quaternary and is distinguished from episodes 1 and 2 by intermediate intraplate-arc-like affinities and consists of widespread basaltic volcanism in Payenia (e.g. Bermúdez et al., 1993; Søager et al., 2013). Payún Matrú, Payún Liso and Auca Mahuida were all constructed during this episode and the young lava flows of the Río Grande Group are attributed to episode 3 based on new geochronological data.

There are several contributions dealing with the geochemistry of the basaltic volcanism of Payenia (e.g. Bermúdez et al., 1993; Saal, 1994b; Nullo et al., 2002; Bertotto et al., 2009; Gudnason et al., 2012; Søager et al., 2013) but the Palaoco plateau and monogenetic cones of Fortunoso have not previously been investigated in detail. The Palaoco lavas show a characteristic arc type geochemical signature (e.g. Ba/La = 20–110) that is absent both prior and following the emplacement of the Palaoco lavas. The presence of arc-type components in the present back-arc during the Late Miocene suggests that the geometry of the subducting slab changed before and after the emplacement of the Palaoco lavas. Initial support for changing slab geometry beneath the Neuquén Basin comes from a compositional study of Pliocene to Holocene primitive basaltic rocks erupted between 35°S and 37°S, 50–250 km east of the arc front (Saal, 1994a) and has since been supported by several other studies (e.g. Kay et al., 2006b). We present evidence that the temporal trends are best explained by steepening of the subduction angle of the Nazca plate, e.g. hypersthene to nepheline normative compositions; lower to higher incompatible trace element content and more to less arc-like incompatible trace element ratios occurring after or during the emplacement of Palaoco and prior to the eruption of Río Grande lavas.

2. Geological setting

Miocene magmatism was widespread in the back-arc of the Andean Southern Volcanic Zone, north of the Cortaderas lineament in the provinces of Mendoza and Neuquén (e.g. Nullo et al., 2002; Sruoga et al., 2008; Spagnuolo et al., 2012) (Fig. 1). Among the volcanic centers that erupted roughly 450 km east of the Chile Trench are the Early Miocene monogenetic cones at Sierra Fortunoso and lava flows and the extensive Late Miocene lavas at Sierra de Palaoco, near 36°S. Petrological characteristics of the dominantly hornblende-bearing basaltic andesite to andesitic complexes of Palaoco are in sharp contrast to those of early Miocene alkaline olivine basaltic flows. Previously, these volcanic

Table 1
Results of $^{40}Ar/^{39}Ar$ analysis of groundmass separates.

Sample	Group	Plateau age				Inverse isochron age			Total fusion age	Geographical position	
		N/N^{tot}	Age ± 2σ Ma	^{39}Ar (%)	MSWD	Age ± 2σ Ma	$^{40}Ar/^{36}Ar$	MSWD	Age ± 2σ Ma	S	W
Miocene Palaoco											
127026	Late	11/11	7.51 ± 0.12	100.0	3.76	7.44 ± 0.08	301 ± 5	3.70	7.57 ± 0.12	36°00.410′	69°23.941′
127020	Late	8/11	7.48 ± 0.19	68.2	0.98	8.00 ± 0.30	287 ± 4	0.55	7.50 ± 0.20	36°00.514′	69°24.104′
127008	Early	4/11	8.30 ± 0.20	37.3	1.68	8.33 ± 0.09	288 ± 4	1.80	8.40 ± 0.20	35°49.800′	69°28.637′
Fortunoso Gr.											
127037	II	7/12	8.62 ± 0.17	67.3	0.32	8.70 ± 0.20	291 ± 6	2.60	8.10 ± 0.20	36°12.957′	69°23.291′
127117	I	3/11	20.70 ± 0.30	31.8	1.66	20.76 ± 0.16	316 ± 6	5.00	21.20 ± 0.20	36°14.059′	69°25.570′
Pliocene–Pleistocene											
127092	Río Grande	7/11	2.87 ± 0.05	80.9	1.43	2.98 ± 0.06	281 ± 8	1.00	2.79 ± 0.06	35°59.176′	69°42.479′
123915	Río Grande	9/11	0.72 ± 0.17	80.9	1.27	0.70 ± 0.20	294 ± 4	2.30	n.c.	36°02.055′	69°43.607′

Accepted ages are underlined. Also given is the number of increments included in the age calculation, % of ^{39}Ar released from the sample and included in the age calculation and Mean Square Weighted Deviation (MSWD) for plateau and isochron age calculations. For the inverse isochron calculation the $^{40}Ar/^{36}Ar$ ratio is also given. Total fusion ages are reported for most samples and geographic locality is quoted in degrees decimal minutes (dd°mm.mmm′). See text for further discussion. n.c. = Not calculated.

areas have been investigated with special attention to geochronology, volcanology, stratigraphy and tectonics (e.g. Giambiagi et al., 2008; Silvestro et al., 2009). Other principal occurrences of Miocene volcanic rocks in Payenia are in the far back-arc are Chachahuen (Kay et al., 2006b), Matancilla and Huantraico (Kay and Copeland, 2006; Dyhr et al., 2013) and Cerro Plateado and surroundings (Litvak et al., 2008, 2009, 2010) and in the present retro-arc area of the Southern Volcanic Zone at 34–37°S Cura Mallín Formation (Kay et al., 2006a), the larger Cajón de Molle area (Nullo et al., 2002; Spagnuolo et al., 2012) and around Cordón del Burrero (Sruoga et al., 2008) Post-Miocene flows are associated with the extensive Llancanelo, Payún Matrú and Auca Mahuída alkaline volcanic fields that cover a vast area of the back-arc (e.g. Bermúdez et al., 1993; Hernando et al., 2012, Kay et al., 2006a, Søager et al., 2013) and are geochemically and petrologically easily distinguishable from the Palaoco rocks. The Río Grande lavas, mainly erupted along the Grande River, are also of post-Miocene age. The NW–SE striking structural feature termed the Cortaderas lineament, located south of Tromen and Auca Mahuída volcanoes, divides the back-arc into two regions: 1) North of the lineament back-arc volcanism is widespread throughout the Miocene to Holocene and 2) south of the lineament, back-arc volcanism is nearly absent and Miocene deformation is insignificant (Ramos, 1978; Nullo et al., 2002; Kay et al., 2006a; Ramos and Kay, 2006; Ramos and Folguera, 2011). Kay et al. (2006a) suggested that the Cortaderas lineament marks the southern boundary of a flat slab region and a period of flat slab subduction was inferred between 17 and 5 Ma (Kay et al., 2006b; Ramos and Kay, 2006; Galland et al., 2007; Folguera and Ramos, 2011; Ramos and Folguera, 2011; Dyhr et al., 2013). An extensional tectonic regime existed in both arc and back-arc in the Oligocene (Folguera et al., 2009) and was possibly caused by the decelleration of the absolute motion of the South American plate after 30 Ma (Silver et al., 1998) and increase in the rate of hinge roll-back of the subducting Nazca plate (Oncken et al., 2006). In the Miocene the continental plate increased its speed (Silver et al., 1998) and hinge roll-back slowed (Oncken et al., 2006), and this could have led to compression and slab shallowing. However, many other factors influence the descent of the Nazca plate such as subduction of fracture zones with enhanced alteration and variation in plate age and speed (e.g. Oncken et al., 2006; Folguera et al., 2011). Our study area is defined to the south by the recent volcanic complex of Payún Matrú. The Palaoco lavas were erupted in this depressed area between the uplifted regions of the Principal Cordillera and the San Rafael Block (Llambías et al., 2010). East of the Principal Cordillera where the Choiyoi Group constitute the basement of the region, the Malargüe fold-and-thrust belt was generated in the Miocene during compression of the Neuquén basin (Ramos and Kay, 2006; Giambiagi et al., 2008). Sierra del Palaoco is part of this belt but no basement crops out in the Palaoco Valley. The stratigraphy of the San Rafael Block to the east consists of Precambrian metamorphic basement unconformably overlain by lower Paleozoic sediments. A thick succession of felsic volcanic rocks related to the Gondwana magmatism was emplaced during the Permo-Triassic (Choiyoi Group), which might also be present below the Palaoco region (Kay et al., 1996; Ramos and Kay, 2006; Llambías et al., 2010).

3. Analytical methods

3.1. $^{40}Ar/^{39}Ar$ age determinations

Samples for radiometric dating were crushed to a 250–400 μm size fraction and were cleaned in a 1% chloric acid solution to remove possible traces of weathered material. To make the contribution of magmatic argon and weathered phases negligible, phenocrysts were removed using magnetic separation methods and finally handpicking under optic microscope, leaving only groundmass to be analyzed. Ar was measured from at least two different aliquots of the same mineral preparation. The $^{40}Ar/^{39}Ar$ geochronology laboratory at the University of Lund uses a Micromass 5400 mass spectrometer with a Faraday and an electron multiplier. A metal extraction line, containing two SAES C50-ST101 Zr–Al getters and a cold finger cooled to app. −155 °C by a Polycold P100 cryogenic refrigeration unit is equipped. Samples were loaded into a copper planchette that consists of several 3 mm holes and step-heated using a defocused 50 W CO_2 laser. Sample clean-up time is 5 min (using the two hot Zr–Al getters and the cold finger). The laser was rastered over the samples to provide even heating of all grains. The analytical process is automated and runs on a Macintosh-steered OS 10.2 with software modified specifically for the laboratory at the University of Lund. Time zero regressions were fitted to data collected from 10 scans over the mass range 36 to 40. Peak heights and backgrounds were corrected for mass discrimination, isotopic decay and interfering nucleogenic Ca-, K-, and Cl-derived isotopes. Blanks were measured before each sample and after every three sample steps. Blank values were subtracted from the sample signal for all incremental steps. Age plateaus were determined following the criteria of Dalrymple and Lanphere (1971), specifying the presence of at least three contiguous incremental heating steps with statistically indistinguishable ages and constituting more than 50% of the total ^{39}Ar released during the experiment. Results are presented in Table 1.

3.2. Major and trace elements

Major element analyses were performed at the Geological Survey of Denmark and Greenland (GEUS) following the method described by Kystol and Larsen (1999). The analytical precision of the data is (1σ, absolute wt.%) SiO_2: 0.15, TiO_2: 0.015, Al_2O_3: 0.05, $Fe_2O_3^{tot}$: 0.1, MnO: 0.003; MgO: 0.05, CaO: 0.03, Na_2O: 0.05, K_2O: 0.005, P_2O_5: 0.005, volatiles; 0.1. Trace element measurements were also performed at GEUS

by inductively coupled plasma mass spectrometry (ICP-MS). Major and trace element data for selected representative samples are in Table 2 and a full data set can be found in electronic Appendix A. The international standards BHVO-2 and BCR-2 and internal standard DISKO-1 were used to monitor the analytical quality and were dissolved and analyzed along with the samples. The precision of trace element analyses is better than 3% (1σ). Results of internal and international standards are listed in Appendix B. Fe^{3+} / (Fe^{3+} + Fe^{2+}) have not been determined analytically and we assume a value of 0.3 for arc-like samples and a value of 0.2 for alkaline lavas. CIPW norms are in electronic Appendix C.

3.3. Nd–Sr–Pb isotopic analyses

Alteration of rocks and contamination during preparation (crushing and grinding) may result in disturbance of the isotopic compositions of basalts, especially Pb isotopes whereas the isotopic composition of relatively immobile elements such as Nd is considered to be resistant to alteration. To avoid the chemical disturbance caused by alteration and possible contamination during sample handling, careful acid leaching of samples prior to dissolution and analysis has been performed. Samples were leached at 125 °C for 1 h in 6 N HCl in closed beakers (leaching time was reduced for samples containing glass). All chemical digestion and separation and the mass spectrometric analyses were performed at the Department of Geography and Geology, University of Copenhagen. All dilutions were made using 18.2 MΩ cm de-ionized water (MQ water) and all lab ware was acid-washed prior to use. The supernatant (leachate solution) was decanted without centrifugation to ensure removal of the silt fraction, which is mostly dominated by secondary alteration phases. The residual sample was rinsed repeatedly with MQ H_2O. Following sequential HF–HNO_3, HNO_3 and HCl–HBr digestion and evaporation the supernatant was subjected to standard double-pass anion exchange chemistry with elution of matrix in 1.5 N HBr + 2 N HCl and collection of Pb with 3 ml 8 N HCl. Column separation for Pb is performed in acid-leached disposable pipette tips loaded with ~0.1 ml of anion exchange resin. Sr was extracted using a cut from 2 N HCl passing through the anion exchange columns and cleaned using Sr-spec©. REE were collected from the columns after Sr and Nd were then extracted from the REE fraction by ion-exchange on Teflon-coated resin using 0.25 N HCl. All isotopic ratios were measured on a VG54-30 thermal ionization mass spectrometer (TIMS) on single Re (Sr, Pb) or double Re–Ta (Nd) filaments. Pb was loaded in silica gel and phosphoric acid and run in the static mode with filament temperatures of 1180–1270°. One or two NBS981 standards were run with each Pb sample batch. The running mean throughout the analyzing period (2010–2012) for NBS981 was 16.9390 ± 0.0029, 15.4992 ± 0.0038 and 36.7234 ± 0.0117 for $^{206}Pb/^{204}Pb$, $^{207}Pb/^{204}Pb$ and $^{208}Pb/^{204}Pb$ respectively (quoted at the 2σ confidence level and N = 35). Total chemical procedure blanks were 50–200 pg, insignificant compared to ~6 ng dissolved sample Pb. Precision of the analyses was better than 100 ppm SEM (standard error of the mean) and better than 50 ppm SEM for most samples. Sr was loaded in 1 N phosphoric acid and Nd was loaded in 0.1 N HCl. Both Sr and Nd were run dynamically with a three-peak jump sequence. Sr and Nd isotopic compositions were exponentially corrected for mass fractionation using $^{86}Sr/^{88}Sr = 0.1194$ and $^{146}Nd/^{144}Nd = 0.7219$, respectively. ^{87}Rb interference on Sr was corrected using ^{85}Rb and ^{144}Sm on Nd using ^{147}Sm. The mean of 53 runs of JNdi and 60 runs of NBS987 during the analyzing period (2010–2012) 0.512096 ± 0.000016 (2σ) and 0.710241 ±0.000019 (2σ). Isotopic ratios of Pb, Sr and Nd are presented in Table 3.

4. Field relations and petrology

The products of two different eruption styles dominate the morphology of the study area (35°50′S–36°15′S). To the north the massive, relatively horizontal sheet flows of Sierra de Palaoco cover an estimated 500 km^2, whereas small monogenetic cones dominate the southern part of the studied area, at Sierra Fortunoso. According to Nullo et al. (2002) both occurrences belong to the Palaoco basalts of the 10–20 Ma Molle Eruptive Cycle. However, Silvestro et al. (2009) use the term Palaoco Formation as defined by Dessanti (1973) for the basalts high in Sierra Palaoco and note that this nomenclature deviates from the original by Groeber (1946). Interspersed throughout the area are younger lava flows which we term the Río Grande Group.

The northern, massive lava flows constitute the Sierra de Palaoco and two profiles have been collected at two different locations covering a large part of the volcanic sequence. Individual lava flows range in thickness from a few to 20 m and at least 30 flows are exposed in the two profiles combined testifying to a voluminous eruption cycle. The Palaoco Volcanic Field is divided into three main areas; Northern, Central and Southern (the latter is further divided into Group I and II based on geochemical affinities) (Fig. 1). The Northern and Central groups constitute the two main profiles, whereas the Southern Group includes a range of monogenetic cones and lava flows erupted along an east–west segment. They all would be expected to be part of the Palaoco Formation according to the map of Silvestro et al. (2009), and we refer to these as the Palaoco Group or simply Palaoco.

A large number of monogenetic cones and related lava flows are found in the area between Sierra de Palaoco and Payún Matrú. We refer to these as the Fortunoso group. The cones of Fortunoso are erupted along two NE–SW trending segments. The degrees of erosion of the western-most of these cones are higher than the eastern cones and the two segments are referred to as Fortunoso I and II, respectively.

Lava flows, not related to either Palaoco or Fortunoso, were collected from the Palaoco Valley and along the Río Grande and are referred to as the Río Grande Group (Fig. 1). Lavas belonging to the Llancanelo Volcanic Field are also collected in the Palaoco Valley, and can petrographically and geochemically be distinguished from Río Grande lavas.

Petrographic differences highlight the geographic division of the large lava sheets of Palaoco and the monogenetic cones of Fortunoso. All Palaoco lavas have phenocrysts of plagioclase + clinopyroxene + Fe–Ti-oxides + amphibole ± olivine. The lower parts of the Palaoco profile (exposed in the Northern profile) are extremely phenocryst rich (40–60 vol.%). Plagioclase is by far the most abundant phenocryst phase, most grains are tabular, 0.5–2 mm in length, un-zoned and appear fresh. Clinopyroxene occurs in all samples as anhedral grains, <1 mm. The lower Palaoco samples differ from the upper Palaoco lavas in having relatively abundant olivine (~2–10 vol.%) and scarce amphibole (<1 vol.%). Olivine phenocrysts are an- or euhedral and <1 mm in diameter whereas amphibole and Fe–Ti-oxide crystals are even smaller. The upper part of the Palaoco profiles (exposed in the central profile and the upper parts of the northern profile) have less than 20 vol.% phenocrysts, mainly plagioclase, accompanied by olivine, amphibole, Fe–Ti-oxides and rare clinopyroxene. The monogenetic cones, constituting the Southern Palaoco group, are divided into two groups based on petrography, one with extremely abundant phenocrysts, common clinopyroxene and scarce amphibole, referred to as the Southern Group I and resembling the lower parts of the northern profile. In contrast to this group, Southern Group II has more abundant amphibole, and resembles the central profile lavas. The groundmass in all Palaoco lavas consists of plagioclase, olivine, clinopyroxene, Fe–Ti-oxides and sometimes glass.

Samples of the Fortunoso cones have less than 10 vol.% phenocrysts, mainly olivine + plagioclase + clinopyroxene. Olivine phenocrysts are mainly subhedral with a maximum size of 5–7 mm. They are commonly replaced partially by iddingsite. Plagioclase crystals are eu- or subhedral with a maximum length of 7–8 mm. Clinopyroxenes are typically anhedral and 1–2 mm in diameter. Fe–Ti-oxides are also common and the groundmass is primarily plagioclase. There are no petrographic differences between Fortunoso I and II.

Río Grande and Llancanelo lavas contain 5–20 vol.% phenocrysts, mainly plagioclase accompanied by abundant olivine and/or amphibole

Table 2
Selected major and trace elements.

Sample	127038	127039	127116	127117	127119	127037	127109	127118	127006	127008	127107
Group	Fortunoso I	Fortunoso I	Fortunoso I	Fortunoso I	Fortunoso I	Fortunoso II	Fortunoso II	Fortunoso II	Palaoco (Early)	Palaoco (Early)	Palaoco S. I
SiO_2 (wt.%)	47.84	45.8	48.16	48.54	48.03	47.04	48.9	47.48	60.6	59.35	58.7
TiO_2	2.37	2.28	2.28	2.57	2.27	1.38	1.91	1.93	0.71	0.81	0.79
Al_2O_3	15.26	12.91	15.03	14.88	14.81	17.42	15.84	14.66	18.03	17.5	18.44
FeO^{tot}	10.37	13.02	11.41	11.97	10.98	10.1	10.77	11.27	4.95	5.78	5.63
MnO	0.16	0.19	0.15	0.17	0.16	0.17	0.16	0.17	0.08	0.1	0.13
MgO	5.27	9.18	6.78	5.78	6.3	7.98	7.47	6.74	2.29	2.8	2.52
CaO	11.28	9.71	9.21	8.43	10.06	10.42	8.95	11.38	6.68	7.07	7.02
Na_2O	4.07	3.53	3.68	3.59	3.97	2.75	3.65	3.6	4.08	4.01	4.04
K_2O	1.62	1.34	1.45	1.99	1.58	1.24	0.88	1.07	1.8	1.7	1.77
P_2O_5	0.6	0.59	0.57	0.74	0.62	0.38	0.27	0.46	0.22	0.22	0.34
Sum	98.85	98.55	98.73	98.67	98.78	98.88	98.8	98.75	99.45	99.36	99.37
$Fe_2O_3^{cor}$	1.92	2.41	2.11	2.22	2.03	1.87	1.99	2.09	1.27	1.48	1.44
FeO^{cor}	8.64	10.85	9.51	9.98	9.15	8.41	8.97	9.39	3.81	4.45	4.33
LOI	3.1	2.7	2.0	3.6	3.1	2.0	0.8	3.2	1.1	0.4	1.4
Sc (ppm)	20.96	17.29	19.41	17.60	16.43	33.60	21.66	9.38	13.17	15.60	12.71
V	187.40	152.96	194.44	193.92	169.07	290.65	190.92	101.96	146.05	162.82	150.91
Cr	232.05	248.35	271.75	216.37	225.34	195.94	213.73	125.08	6.02	8.14	1.36
Co	40.16	59.92	48.83	47.13	46.65	40.36	43.00	23.46	14.31	17.37	16.48
Ni	83.42	278.08	201.41	183.05	192.29	84.55	104.52	88.63	8.54	11.74	8.68
Cu	47.29	59.99	55.24	46.71	48.13	53.56	42.74	28.01	23.24	20.59	30.31
Zn	95.68	103.91	110.70	116.47	107.04	64.89	92.62	48.95	52.51	48.83	59.14
Ga	23.56	20.80	22.92	23.83	22.24	19.51	20.45	10.17	20.03	19.09	20.65
Rb	13.86	11.69	10.72	14.86	13.61	25.84	10.13	5.39	42.58	40.45	55.09
Sr	782.93	603.98	765.91	920.50	815.97	792.77	491.44	292.40	1051.16	907.11	912.65
Y	20.53	23.04	20.50	21.60	19.44	22.54	20.13	9.97	11.23	13.36	17.07
Zr	201.16	163.54	198.27	236.90	205.15	92.12	111.90	75.28	106.33	97.90	125.32
Nb	31.06	30.67	31.92	41.95	33.61	7.05	11.98	10.17	7.17	5.25	6.87
Cs	0.22	0.11	0.12	0.15	0.11	3.67	0.09	0.05	1.24	1.92	3.00
Ba	336.06	636.45	242.32	345.33	294.19	332.82	254.29	148.28	1075.39	988.78	938.29
La	23.25	22.79	21.33	27.62	23.75	14.47	11.82	9.00	16.33	14.45	19.19
Ce	50.47	48.67	45.43	57.73	50.69	33.11	26.33	18.80	30.77	29.39	37.99
Pr	6.43	6.20	5.82	7.24	6.34	4.57	3.52	2.41	3.43	3.42	4.98
Nd	27.31	26.88	25.90	32.12	27.87	20.52	16.31	10.68	13.96	14.37	20.22
Sm	6.24	6.36	5.71	6.94	6.00	5.02	4.25	2.44	2.69	3.08	4.30
Eu	2.02	1.93	1.97	2.30	2.05	1.59	1.47	0.84	0.79	0.94	1.20
Gd	5.89	6.01	5.69	6.66	5.81	5.01	4.42	2.54	2.53	2.91	3.90
Tb	0.821	0.868	0.826	0.900	0.814	0.776	0.657	0.365	0.360	0.422	0.539
Dy	4.45	4.66	4.19	4.68	4.14	4.35	3.70	2.01	1.94	2.33	3.01
Ho	0.763	0.825	0.740	0.770	0.720	0.818	0.740	0.360	0.390	0.450	0.580
Er	1.93	2.18	1.82	1.97	1.78	2.27	1.90	0.93	1.06	1.28	1.61
Tm	0.263	0.305	0.250	0.250	0.240	0.341	0.270	0.130	0.160	0.180	0.220
Yb	1.50	1.70	1.44	1.45	1.32	2.07	1.62	0.74	1.00	1.12	1.42
Lu	0.203	0.236	0.200	0.210	0.190	0.298	0.240	0.120	0.160	0.160	0.230
Hf	4.52	4.06	4.45	5.31	4.51	2.53	2.77	1.76	2.92	2.62	3.07
Ta	1.814	1.789	1.870	2.476	1.963	0.416	0.667	0.575	0.474	0.305	0.432
Pb	2.47	2.11	2.21	2.48	2.28	3.66	2.34	0.97	11.79	9.09	11.54
Th	2.04	1.79	1.96	2.48	2.04	2.49	1.29	0.82	4.17	2.53	4.35
U	0.697	0.350	0.490	0.770	0.480	0.719	0.190	0.290	1.730	1.010	1.670

and scarce clinopyroxene and Fe–Ti oxides. Plagioclase crystals mostly occur as zoned tabular crystals reaching 1–3 mm in length. Amphibole is common in Río Grande Group but absent in Llancanelo. When present, amphibole occurs as anhedral grains, seldom reaching more than 1 mm in diameter. Fe–Ti-oxides are often surrounded by amphibole. Clinopyroxene is rare but occurs as partially dissolved phenocrysts. The groundmass is composed of plagioclase, clinopyroxene, olivine and glass.

5. Geochronology

All radiometric analyses are shown in Table 1 and age plateaus are shown in Fig. 2. We present the radiometric results in chronological order, describing the oldest rocks first. All errors of the age data are reported at the 2σ confidence level.

5.1. Fortunoso

A single sample from the western cones of Fortunoso was analyzed and has a plateau age of 20.70 ± 0.30 Ma and an isochron age of 20.76 ± 0.16. Only 30% of the cumulative released ^{39}Ar is included in the plateau calculation, however, the age is supported by the total fusion age (21.20 ± 0.20 Ma). The $^{40}Ar/^{36}Ar$ is slightly higher than the atmospheric component (316 ± 6) indicating that 20.76 ± 0.16 should be considered a maximum age. Silvestro et al. (2009) reported 250 m of basalts of Early Miocene age (estimated from a disturbed Ar-spectrum to c. 24 Ma) at the western slopes of Sierra de Palaoco, the Cerrillos Formation, but Early Miocene ages has not previously been detected to the east of the ridge. The Cerrillos Fm. is distinctly older than the Molle Fm. of app. 18 Ma (Silvestro et al., 2009).

Sample 127037 from a volcanic cone in the oilfield to the north of Payún Matrú belongs to the eastern segment of monogenetic cones

127108	127114	127020	127021	127023	127026	127011	127034	127106	127030	127031	127032	127033
Palaoco S. I	Palaoco S. I	Palaoco (Late)	Palaoco (Late)	Palaoco (Late)	Palaoco (Late)	Palaoco (Late)	Palaoco S. II	Palaoco S. II	Río Grande	Río Grande	Llancanelo	Llancanelo
67.73	63.12	54.04	54.27	48.63	57.06	58.69	57.96	53.36	55.68	57.17	48.62	48.12
0.37	0.59	0.9	0.86	1.21	0.66	0.81	0.91	1.18	0.82	0.74	1.67	1.63
17.01	17.27	18.17	19.85	18.51	19.56	17.34	18.2	17.73	18.29	18.41	17.25	15.83
2.65	4.4	7.52	6.96	9.67	5.77	6.08	5.8	7.73	6.7	6.82	9.63	10.41
0.03	0.09	0.19	0.15	0.2	0.16	0.15	0.18	0.18	0.21	0.2	0.16	0.16
1.32	2.25	3.3	2.47	4.69	1.72	2.54	1.8	2.34	2.94	2.91	6.07	8.62
4.33	5.42	8.23	7.65	10.54	6.85	6.84	4.64	8.21	7.77	6.66	10.69	8.98
4.31	3.91	4.14	4.29	3.32	4.77	4.21	5.49	4.54	4.24	3.75	3.49	3.72
1.77	2.24	2.18	2.25	1.7	2.28	2.37	3.88	3.23	2.23	2.17	0.95	1.02
0.17	0.22	0.49	0.49	0.46	0.52	0.3	0.49	0.64	0.38	0.42	0.4	0.35
99.71	99.51	99.16	99.22	98.92	99.36	99.32	99.35	99.14	99.25	99.24	98.93	98.84
0.68	1.13	1.93	1.79	2.48	1.48	1.56	1.49	1.98	1.72	1.75	1.78	1.93
2.04	3.38	5.78	5.35	7.44	4.44	4.68	4.46	5.95	5.16	5.24	8.02	8.67
2.6	1.4	1.6	0.8	1.0	1.3	1.7	0.4	2.1	4.1	4.8	1.6	0.0
7.08		14.94		22.44	14.85	14.18	18.34	14.23	9.80	8.96	27.13	24.84
81.14		165.78		267.67	77.77	128.79	59.02	140.23	135.73	99.70	217.36	201.69
9.56		10.13		8.84	0.69	31.82	0.94	0.47	8.51	0.85	108.11	246.64
6.67		19.72		29.17	11.38	15.38	8.59	18.15	16.03	14.50	37.09	47.49
9.45		11.71		16.67	2.53	18.37	2.39	6.71	7.03	3.31	43.34	153.76
7.79		31.24		47.85	13.95	26.83	10.17	40.42	20.98	18.16	45.05	40.80
29.32		72.52		69.66	53.53	63.18	46.82	73.42	64.92	61.58	71.46	85.34
16.26		21.10		22.26	22.08	19.99	23.56	22.32	22.22	21.06	20.93	20.57
53.16		56.49		44.96	51.41	64.09	149.23	109.17	64.50	43.96	17.69	21.15
878.08		889.95		907.64	948.53	623.84	591.48	639.36	789.31	742.68	612.56	572.27
7.56		23.60		25.10	24.48	22.53	38.48	36.35	25.06	22.75	24.62	21.68
69.13		164.88		125.72	187.91	204.52	424.73	327.49	163.63	187.33	135.40	121.87
3.81		8.25		6.48	7.96	8.50	20.74	16.35	7.74	7.40	13.56	12.74
1.60		1.70		1.93	0.92	1.33	3.59	1.98	0.89	0.68	0.53	0.81
1244.85		827.64		562.10	908.01	727.28	948.89	835.02	803.21	704.79	378.25	363.48
11.35		30.62		24.67	31.17	28.84	46.97	38.54	31.22	28.17	17.74	17.02
19.76		61.61		52.03	64.51	56.69	100.75	82.26	62.95	59.52	38.63	36.40
2.35		7.59		6.55	7.82	6.87	12.13	10.47	7.75	7.33	4.88	4.63
9.10		30.71		27.94	31.76	26.56	47.84	42.53	30.91	29.22	20.94	19.91
1.71		5.96		6.08	6.07	4.90	9.18	8.45	6.04	5.62	5.01	4.79
0.50		1.79		1.78	1.88	1.39	2.24	2.01	1.75	1.66	1.62	1.50
1.64		5.38		5.66	5.40	4.60	7.95	7.65	5.45	5.07	4.99	4.80
0.233		0.796		0.813	0.767	0.692	1.174	1.117	0.779	0.734	0.748	0.708
1.25		4.34		4.60	4.44	3.90	6.71	6.35	4.29	4.17	4.43	4.08
0.240		0.820		0.877	0.832	0.770	1.294	1.250	0.848	0.773	0.821	0.766
0.68		2.34		2.36	2.45	2.20	3.77	3.53	2.45	2.29	2.26	2.00
0.100		0.340		0.366	0.384	0.360	0.582	0.530	0.376	0.339	0.340	0.285
0.65		2.20		2.33	2.47	2.25	3.84	3.41	2.51	2.23	2.11	1.85
0.100		0.330		0.338	0.380	0.360	0.563	0.530	0.359	0.333	0.293	0.255
2.00		4.03		3.20	4.44	5.02	9.38	7.58	4.08	4.44	3.19	3.09
0.252		0.452		0.354	0.463	0.539	1.169	0.970	0.454	0.425	0.719	0.703
11.55		8.48		6.78	8.78	12.35	9.65	11.56	9.05	7.00	3.23	4.02
1.95		6.08		4.83	6.39	9.05	19.16	16.53	7.46	5.63	2.29	2.72
1.110		1.550		1.254	1.751	2.250	4.228	3.890	2.128	1.666	0.602	0.701

and reveals a plateau age of 8.62 ± 0.17 Ma in accordance with the inverse isochron age of 8.70 ± 0.20 Ma. The plateau constitutes approximately 70% of the released ^{39}Ar and the $^{40}Ar/^{36}Ar$ ratio of 291 ± 6 is in agreement with an atmospheric component. The plateau-age is accepted as the geologic age of the monogenetic cone.

5.2. Palaoco

Radiometric ages have been obtained for three samples from the Palaoco Volcanic Field. The three samples are all from the massive lava flows constituting the bulk of the Palaoco plateau. The strongly eroded cliffs provide an excellent opportunity to investigate the magmatic evolution through an extended period of time. Sample 127008, belongs to the lower parts of the Palaoco profile (exposed in the cliffs of our northern Palaoco profile) and gives a plateau age of 8.30 ± 0.20 Ma constituting only app. 40% of the released argon. The plateau age is confirmed by the inverse isochron age of 8.33 ± 0.09. A slightly low $^{40}Ar/^{36}Ar$ ratio of 288 ± 4 indicates that the age should be considered a minimum age. All lavas similar to 127008 in geochemical affinities are referred to as 'Early Palaoco'. Two slightly younger samples (127020 and 127026) were collected 20 km to the SE in the Central Palaoco profile and reveal ages of 7.48 ± 0.19 Ma and 7.51 ± 0.12 Ma respectively. Both plateaus are well defined. All lavas similar in geochemical composition are referred to as 'Late Palaoco'.

Based on radiometric dating and field relations, cones of the Southern Group I and the lower part of the Northern Palaoco profile are oldest followed by lavas of the Central profile. This stratigraphy is in accordance with field observations as all lavas of the main plateau dip 3–5°E and the central profile is located to the SE of the northern profile. There are no radiometric ages of Southern Group II but based on their geochemical affinities they are inferred to be simultaneous or younger than the Central Group lavas (see Discussion).

A Palaoco basalt from the bottom of the sequence on the western slope of Sierra de Palaoco opposite our central profile was dated by $^{40}Ar/^{39}Ar$ to 8.14 ± 0.12 (2σ) Ma (Silvestro et al., 2009), and this may

represent the oldest part of the same flow sequence analyzed by us. Giambiagi et al. (2008) grouped Middle–Late Miocene rocks into the Huincán Formation (10.5–5.5 Ma). This corresponds to the Huincán II Fm. (7.5–4.8 Ma) of Kay et al. (2006a), and they referred to the Huincán I Fm. with the period 14–11 Ma. Spagnuolo et al. (2012) added The Charilehue Fm. (18–14 Ma) to this scheme and use the interval 10–5 Ma for the Huincán II Fm. cf. Combina and Nullo (2000). Accordingly, the Palaoco and Fortunoso II age information presented here assigns the succession to the Huincán II Fm.

5.3. Río Grande

Several thick lava flows have flown from volcanic centers both east and west of the Río Grande. On the eastern bank of the Río Grande the young lavas of Los Volcanes overlie a thick volcanic sequence, deeply eroded by the river. Between 35°50′S and 36°S, north of Los Volcanes, outcrops of this sequence are plentiful but their origin is unknown. Sample 127092 gives a well defined plateau age of 2.87 ± 0.05, in accordance with an isochron age of 2.98 ± 0.06 Ma. Sample 123915 is collected from a 1.5 km long basaltic lava flow that originates from a small monogenetic cone west of Río Grande. A well-defined plateau, constituting 85.6% of the released argon, gives an age of 0.72 ± 0.17.

6. Geochemistry

Major and trace element compositions for selected samples, representative of all groups, are given in Table 2. As previously mentioned, Palaoco samples are subdivided into three groups; Northern, Central and Southern and it will be shown that the upper lavas of the Northern profile share geochemical affinities with the Central Group. Based on geochemical characteristics we refer to the lower parts of the Northern Group as 'Early Palaoco' and to the upper parts of Northern profile along with the Central Group as 'Late Palaoco'. Fortunoso samples are divided into two groups (I and II) based on major and trace element characteristics (see Fig. 1 for geographic details). Also treated are younger mafic lavas erupted in the Palaoco Valley and along the Río Grande. They are divided into two groups (Río Grande and Llancanelo) on the basis of geography and geochemical characteristics, with the older Río Grande lavas showing a stronger arc signature than the younger Llancanelo lavas.

6.1. Major elements

6.1.1. Palaoco

Major element variation diagrams are presented in Fig. 3. The Early Palaoco rocks show a variation in SiO_2 content from 54.0 to 60.6 wt.%. Slightly lower values of SiO_2 for a given content of MgO are observed in the Late Palaoco samples (50.7–58.5 wt.%). Southern Group I resembles the Early Palaoco rocks in silica content whereas Southern Group II resembles the Late Palaoco rocks in terms of SiO_2, at a given MgO. MgO ranges from ~4.5 to 1 wt.%. Based on the TAS diagram the Early Palaoco and Southern Group II lavas range from basaltic trachyandesites through trachyandesite/andesite to dacite and the Late Palaoco and Southern Group I lavas range from trachybasalt to trachyandesite (Fig. 4a). Late Palaoco lavas become increasingly more potassium rich relative to sodium and evolve from hawaiites/mugearites to shoshonitic compositions (Le Maitre, 2002). Southern Group I lavas generally have higher alkali contents than the Late Palaoco lavas. SiO_2, Na_2O, K_2O content increase and CaO, TiO_2 and FeO^{tot} decrease with decreasing MgO. Al_2O_3 remains constant around 18 wt.% in the Early Palaoco lavas and around 20 wt.% in the Late Palaoco lavas. Noticeable differences in major element content between the Early and Late parts of Palaoco are observed, with the Late Palaoco lavas (along with Southern Group II) showing higher TiO_2, FeO^{tot}, Al_2O_3, CaO, K_2O and P_2O_5 at a given MgO content. K_2O is especially high in Southern Group II lavas which is in contrast to nearby Southern Group I lavas, showing the lowest contents of K_2O (Fig. 4b). Early Palaoco lavas and Southern Group I plot as medium-K rocks in the K_2O–SiO_2 classification diagram for orogenic rocks whereas the Late Palaoco group belongs to the high-K series and the Southern Group II range to shoshonitic compositions (Fig. 4b).

Most Palaoco samples (with the exception of Southern Group I and some Early Palaoco lavas) have slightly higher alkali contents than the local main arc. Almost all Palaoco lavas are hypersthene normative.

6.1.2. Fortunoso

Small volume alkaline basalts and trachybasalts constitute Fortunoso I and II. The monogenetic cones and related lava flows are erupted along two NE–SW striking alignments. The Fortunoso Groups display a limited range in SiO_2 (~45–50 wt.%) and MgO (5–9 wt.%) (Fig. 3). The western cones, Fortunoso I have high TiO_2, FeO^{tot}, K_2O, CaO and P_2O_5 compared to the eastern cones, Fortunoso II. Based on the TAS diagram (Fig. 4a) all Fortunoso I lavas are trachybasalts or basalts and all Fortunoso II lavas are basalts.

Table 3
Isotopic compositions of Sr, Nd and Pb.

Sample	Group	$^{87}Sr/^{86}Sr$	2σ	$^{143}Nd/^{144}Nd$	2σ	$^{206}Pb/^{204}Pb$	$^{207}Pb/^{204}Pb$	$^{208}Pb/^{204}Pb$
127038	Fortunoso I	0.703789	8	0.512861	9	18.275	15.549	38.046
127039	Fortunoso I	0.703694	3	0.512852	10	18.373	15.585	38.205
127116	Fortunoso I	0.703666	10	0.512870	6	17.907	15.325	37.270
127117	Fortunoso I	0.703667	10	0.512868	8	18.343	15.576	38.099
127119	Fortunoso I	0.703744	21	0.512842	5	18.226	15.508	37.928
127037	Fortunoso II	0.704180	4	0.51277	2	18.590	15.603	38.438
127109	Fortunoso II	0.703972	68			18.345	15.587	38.315
127118	Fortunoso II	0.703732	56	0.512805	9	18.328	15.577	38.182
127006	Palaoco (Early)	0.703993	18	0.512754	32	18.560	15.595	38.398
127008	Palaoco (Early)	0.704291	6	0.512692	13	18.506	15.590	38.375
127107	Palaoco (Southern I)	0.704117	4	0.512760	8	18.593	15.602	38.462
127108	Palaoco (Southern I)	0.704422	5	0.512660	3	18.506	15.593	38.369
127114	Palaoco (Southern I)	0.703728	4	0.512851	10	18.219	15.534	38.033
127020	Palaoco (Late)	0.704033	5	0.512733	9	18.597	15.606	38.488
127021	Palaoco (Late)	0.703778	17	0.512807	9	18.605	15.599	38.476
127023	Palaoco (Late)	0.703767	8	0.512817	7	18.628	15.592	38.456
127026	Palaoco (Late)	0.704072	4	0.512761	9	18.583	15.595	38.434
127011	Palaoco (Late)	0.703727	5	0.512933	8	18.529	15.538	38.514
127034	Palaoco (Southern II)	0.704137	4	0.512727	13	18.597	15.607	38.481
127106	Palaoco (Southern II)	0.703860	4	0.512782	7	18.582	15.593	38.444

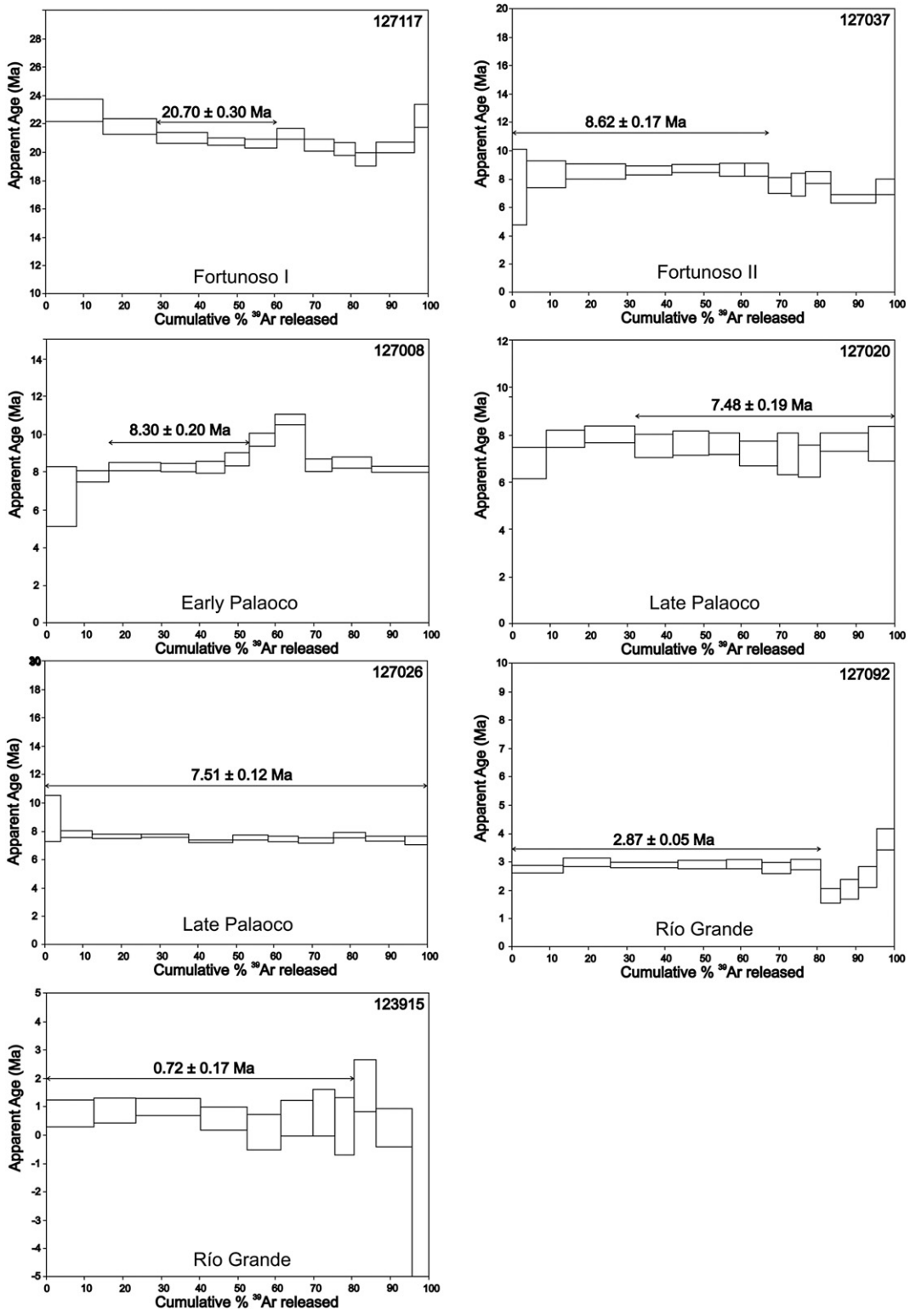

Fig. 2. Results of $^{40}Ar/^{39}Ar$ analysis for Palaoco, Fortunoso and Río Grande lavas. The increments included in the age calculation in the plateau diagrams are indicated with horizontal lines. Calculated ages are reported with a 2σ uncertainty.

6.1.3. Río Grande and Llancanelo

Younger mafic samples, erupted along the Río Grande and in the Palaoco Valley, are divided into two groups based on geochemical characteristics. Río Grande lavas show major element variations similar to Palaoco lavas. They range from basalt to trachyandesite (Fig. 4a) and they plot in the high-K field on the K_2O–SiO_2 classification diagram (Fig. 4b). Llancanelo show more alkaline affinities, similar to Fortunoso Group II with higher SiO_2 and Al_2O_3 at a given MgO and lower TiO_2, FeO^{tot}, K_2O, CaO and P_2O_5 than Fortunoso Group I.

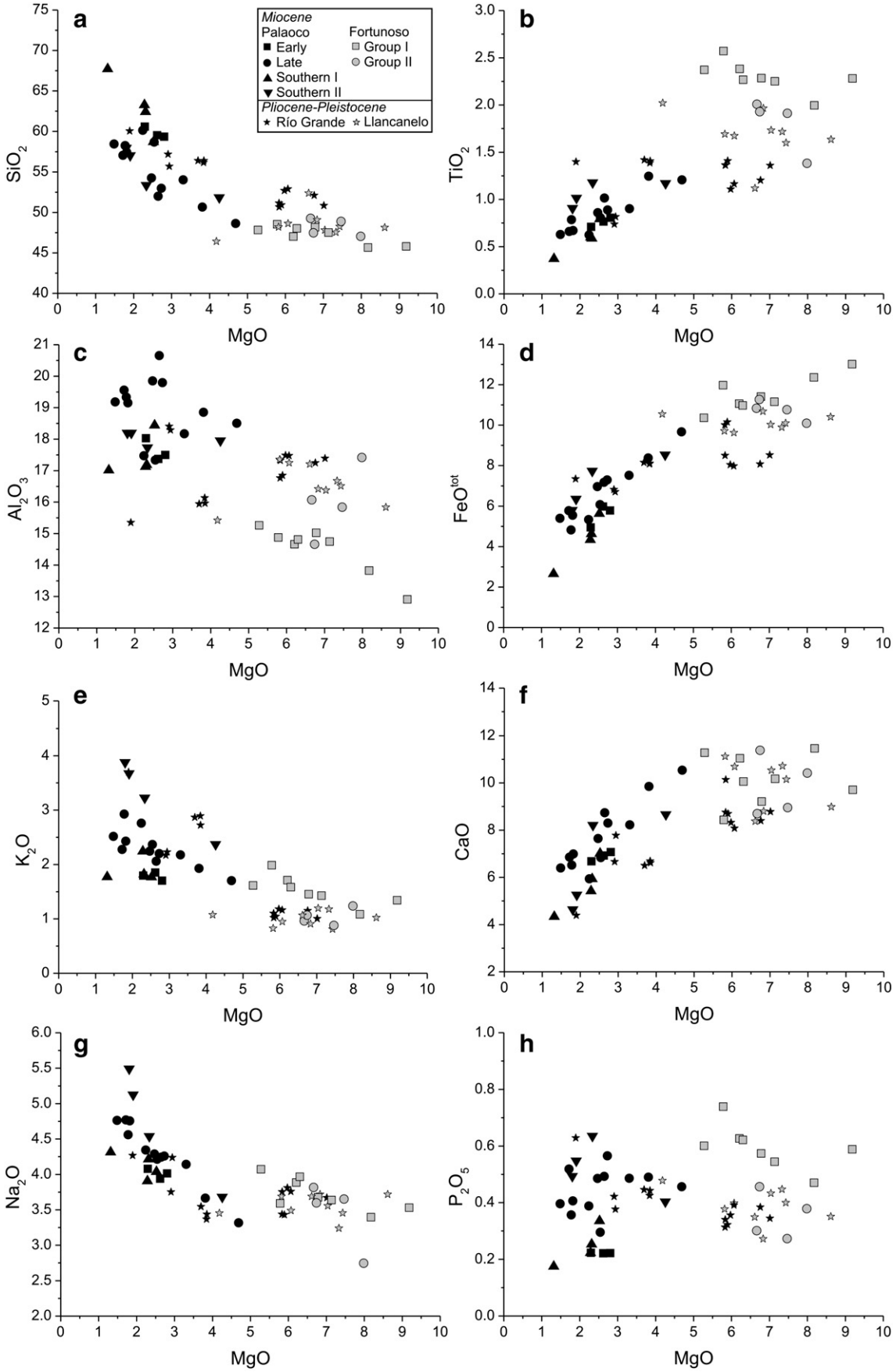

Fig. 3. Major element variation (wt.% oxides) vs. MgO for Palaoco, Fortunoso, Río Grande and Llancanelo rocks. The grouping of the rocks is discussed in the text.

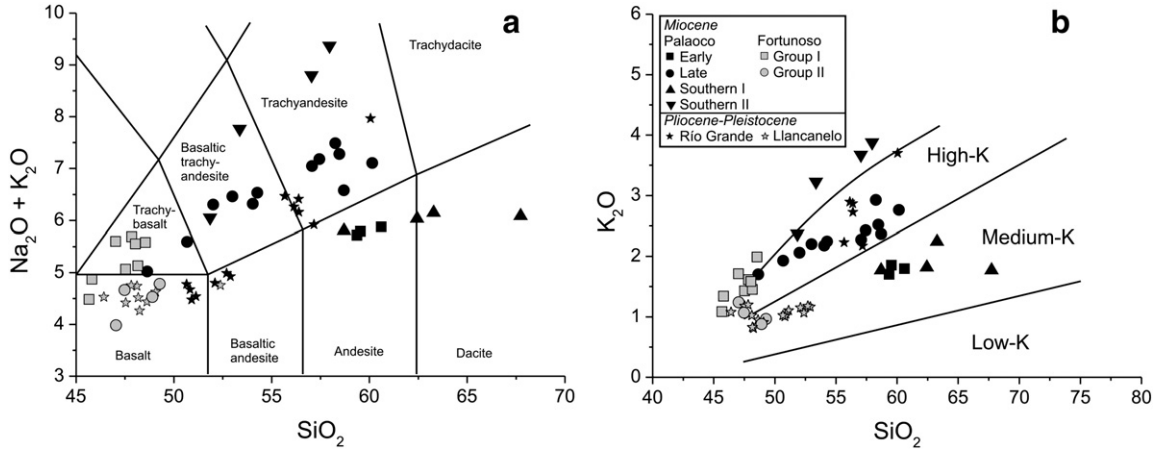

Fig. 4. a) Total alkali vs. silica classification diagram (Le Maitre, 2002) and b) K_2O vs. SiO_2 classification diagram for orogenic rocks.

6.2. Trace elements

6.2.1. Palaoco

Similar to other back-arc high-K rocks (such as Chachahuén (Kay et al., 2006b)), Palaoco rocks have high LIL element concentrations and arc-like trace element characteristics such as arc-like Ba/La ratios (>20) and low Ta to LREE ratios. The volcanic products of Palaoco show relatively high abundances of mantle incompatible elements but only Ba increase throughout the series as MgO decreases (Fig. 5). Southern Group II is characterized by anomalously high Th, Y, Nb, La, Rb and Zr in contrast to the Southern Zone I and Early Palaoco lavas in the northern group which generally show the lowest contents of incompatible elements. Vice versa, Sr is high in the latter two groups, whereas Southern Group II has the lowest Sr of all (Fig. 5). Variations of selected compatible trace elements as a function of wt.% MgO are presented in Fig. 6. Low MgO (<5 wt.%), Ni and Cr concentrations show that all of these lavas are fractionated relative to mantle melts. All Palaoco groups have roughly the same compatible trace element abundance at a given MgO. V decreases dramatically along with Sc with decreasing MgO.

Selected analyses, covering the compositional spectrum, are shown in primitive mantle normalized diagrams (Fig. 7). Compositions for the continental volcanic arc basalts (Laguna del Maule Frey et al., 1984; Holm et al., in preparation) and the local back-arc end member defined by Río Colorado (Søager and Holm, in preparation) are shown for comparison. The arc-like Palaoco lavas are clearly different from the OIB-like Río Colorado lavas in having positive anomalies of Ba and Sr, negative anomalies of Nb and Ta with respect to adjacent elements of similar incompatibility. Within the Palaoco plateau, the Early Palaoco lavas show a distinct negative Th anomaly and generally less enriched trace element patterns compared to the Late Palaoco lavas. REE concentrations (especially those of the middle REE (Sm to Tb)) decrease with increasing SiO_2 content for all Palaoco Groups. Palaoco lavas show relatively flat HREE patterns ($(Tb/Yb)_N = 1.30–1.75$).

Palaoco rocks are easily distinguished from Fortunoso rocks in Ce/Y–Nb/Y space with Palaoco lavas ranging to much higher Ce/Y at low Nb/Y ratios (Fig. 8a). Late Palaoco lavas exhibit the highest Ce/Nb (>6) with other Palaoco groups ranging from 4 to 6. Another major difference between the two southern Palaoco groups is their Th/U ratios that vary from 1.5 to 2.5 in the Southern Group I (similar to the Early Palaoco lavas) and from 3.5 to 4.5 in Southern Zone II (similar to the Late Palaoco lavas) (Fig. 8b).

Samples 127010 and 127111 are the upper, hence youngest, lavas of the northern profile and they share major and trace element characteristics with the Central Palaoco Group, e.g. similar Ce/Pb (4–6) ((Fig. 9) and are therefore treated as 'Late Palaoco'.

Volcanism concomitant with the Palaoco has been recorded from Chachahuén (Kay and Copeland, 2006) and Cerro Plateado and some other nearby volcanic occurrences (Litvak et al., 2008, 2009) in the far back-arc. The enrichment at Chachahuén is rather like that of Palaoco with respect to Ba/La. However, the enrichment in Ba and La compared to Ta is much less and is as in the Southern II group or less (La/Ta in Late Palaoco and Southern Group II ranges from 35 to 70). The northernmost Huincan II volcanism was termed La Brea by Nullo et al. (2002) and has a trace element pattern with considerable resemblance to Early Palaoco ages ranging 7.2–9.4 Ma (5.8 ± 1.8 to 10.7 ± 1.0 Ma if also rather uncertain results are considered), thus overlapping with Palaoco.

6.2.2. Fortunoso

Although Fortunoso Groups I and II are difficult to differentiate in the field, there are several important trace element variations. Fortunoso II has low Nb (<15 ppm), La (<15 ppm), Zr (~100 ppm) and Sr (<500 ppm for most samples) compared to Fortunoso I (Nb: >25 ppm; La: >15 ppm; Zr: 150–250 ppm and Sr: 600–900 ppm) (Fig. 5). There are also low abundances of compatible trace element abundances in Fortunoso II (e.g. Ni and Cr) that are not related to the degree of fractionation affecting the samples (Fig. 6). Primitive mantle normalized diagrams (Fig. 7) show the OIB-like nature of Fortunoso I with positive Sr, Zr and Ti anomalies, lack of negative Nb–Ta anomaly, and the steepest HREE pattern ($(Tb/Yb)_N = 2.24–2.99$). Fortunoso II shows the same features but also a positive Pb anomaly, slightly negative Nb–Ta and flatter HREE patterns. Data from the volcanic arc (Laguna del Maule) and the back-arc OIB-like end member defined as the Río Colorado lavas are included for comparison.

Several incompatible trace element ratios distinguish the two Fortunoso groups: The Th/Ta ratio is ~1 in Fortunoso I, slightly higher in Fortunoso II (1–2) and anomalously high in sample 127037 (~6). Ba/Nb and La/Nb are also elevated above other Fortunoso lavas testifying to the more arc-like qualities of the sample (Fig. 10b). Fortunoso I vary in Nb/Y from 1.3 to 2.0 in contrast to Fortunoso II ranging from 0.3 to 1.0 (Fig. 8) reflecting the relatively high Nb and low HREEs (including Y) in Fortunoso I.

Geochemically as well as temporarily Fortunoso I is comparable to the voluminous La Matancilla lavas (20–24 Ma) constituting a large plateau 50 km to the south (Figs. 1 and 10) (Kay and Copeland, 2006; Dyhr et al., 2013).

6.2.3. Río Grande and Llancanelo

Río Grande lavas have many features in common with Palaoco lavas and tend to be most like Southern Group II with very high Th, Y, La, Rb and Zr and relatively low Sr abundances at a given MgO content. In contrast, Llancanelo lavas show trace element abundances similar to Fortunoso II, with high Th, Ba and Rb along with low Nb, Sr, La, and Zr compared to Fortunoso I (Fig. 5). Compatible trace element abundances confirm the similarity to Fortunoso II with much

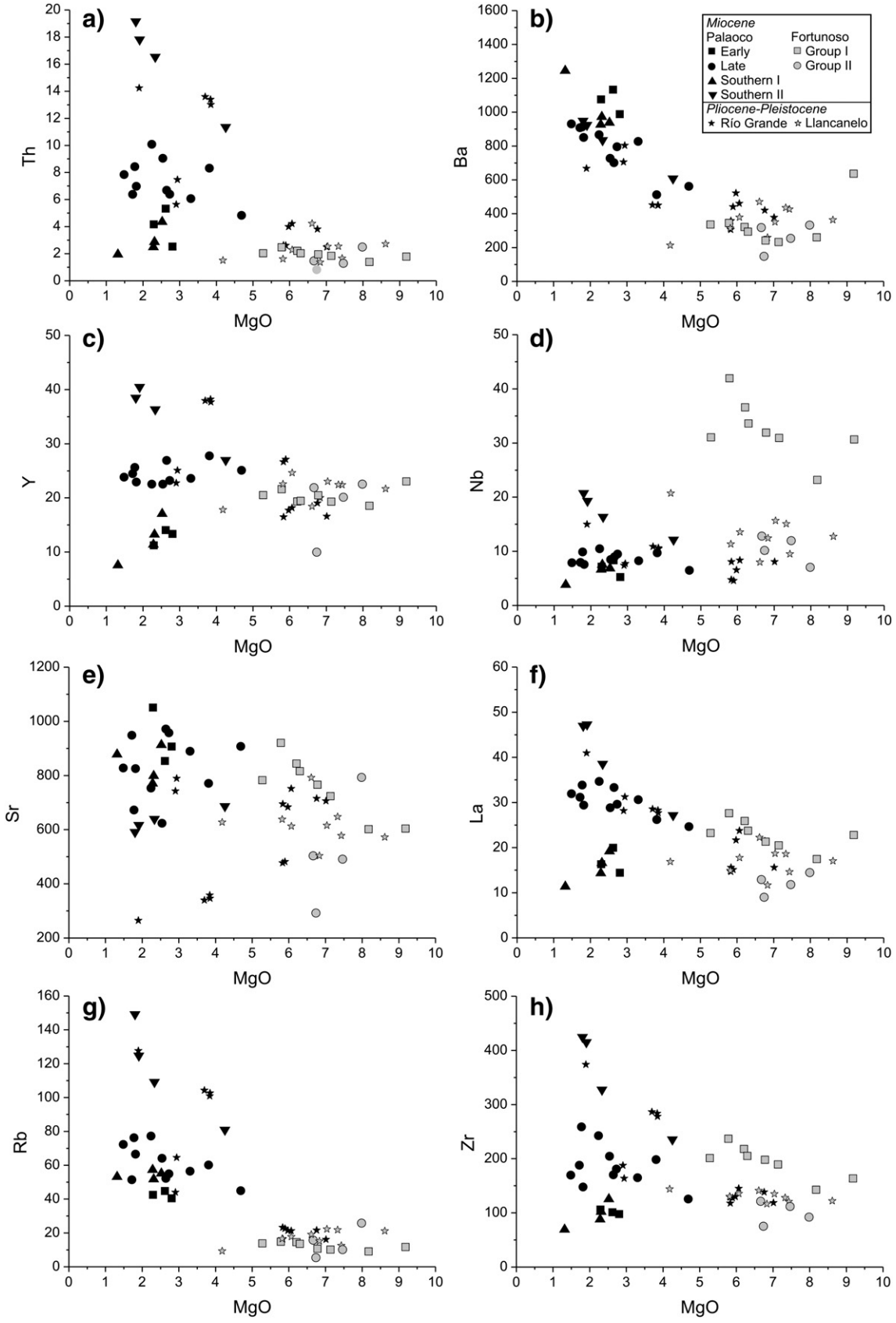

Fig. 5. Incompatible element variation (ppm) vs. wt.% MgO.

lower Ni and Cr and higher Sc and V than Fortunoso I (Fig. 6). Primitive mantle normalized trace element diagrams show the arc-like nature of Río Grande lavas with a negative Nb–Ta anomaly, positive Pb and negative Ti anomalies. Llancanelo rocks shows features of both arc-like and OIB-like character, e.g. a weak to strong negative Nb–Ta anomaly, a strong positive Pb anomaly, but no negative Ti-

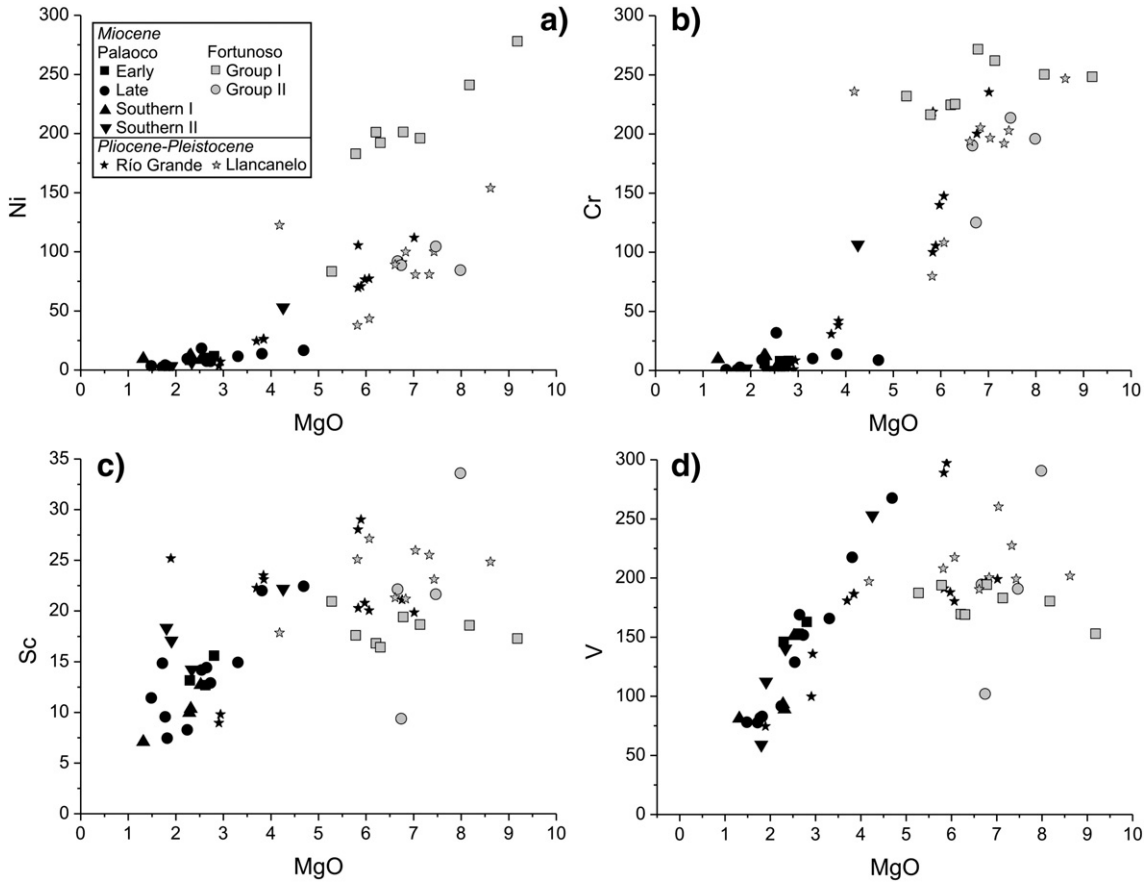

Fig. 6. Compatible trace element variation (ppm) vs. wt.% MgO.

anomaly, an OIB-like LIL element pattern and a steep HREE pattern, similar to Fortunoso lavas (Fig. 7). Río Grande show high Ce/Y at a given Nb/Y similar to Palaoco lavas and Llancanelo show low Ce/Y and Nb/Y ratios similar to Fortunoso II (Fig. 8).

6.3. Isotope ratios

Nineteen samples were analyzed for $^{206}Pb/^{204}Pb$, $^{207}Pb/^{204}Pb$, $^{208}Pb/^{204}Pb$ and $^{87}Sr/^{86}Sr$ isotope ratios, and sixteen samples were analyzed for $^{143}Nd/^{144}Nd$ (Table 3). The Sr isotope composition of the alkaline Fortunoso I cones and lavas ranges from 0.70367 to 0.70379. Three samples from the Fortunoso II group were analyzed and reveal a large span in Sr isotopic ratios (0.70373–0.70418) for this group which has been shown in Section 6.2 to be intermediate between Fortunoso I and Palaoco. Palaoco lavas range from 0.70377 to 0.70442 with Early Palaoco defining the high end of the spectrum and Late Palaoco defining the low end (Fig. 11). Also plotted are data from Río Colorado and Laguna del Maule for comparison. The Nd isotope ratios correlate negatively with $^{87}Sr/^{86}Sr$, ranging for alkaline lavas from 0.51273 to 0.51287 and from 0.51269 to 0.51293 for Palaoco lavas. There is a wide span in Pb isotope ratios between Palaoco and Fortunoso with Palaoco being more radiogenic (Fig. 11). No clear correlation between Sr or Nd and Pb isotopic ratios occur.

7. Discussion

We discuss the magmatic evolution and the relative roles of fractional crystallization and crustal contamination before turning to the systematic changes in mantle melt composition and identify the local end-members that explain the variation. Finally these new results and considerations are evaluated in the light of possible changes in plate tectonic setting.

7.1. Fractional crystallization

Palaoco lavas and cones were erupted over at least 1 Ma and smooth major and trace element variations indicate that crystal fractionation played a dominant role. Fractionating minerals are likely to be the phenocryst phases observed in Palaoco lavas: olivine, clinopyroxene, plagioclase, amphibole and Fe–Ti oxides. The changes in slopes on MgO variation diagrams (Fig. 3) are consistent with a major role for mineral/melt fractionation. MgO correlates with Ni (25–0 ppm) and Cr (10–0 ppm) and Mg# (<55) indicate the relatively evolved nature of Palaoco lavas. Increasing SiO_2 and decreasing Ni and FeO with decreasing MgO is consistent with olivine fractionation, and decreasing TiO_2 indicates that Fe–Ti oxides also fractionated. Increasing Al_2O_3/CaO ratios with decreasing MgO and a good positive correlation between Sr and Ce (not shown) in Late Palaoco indicate that the clinopyroxene/plagioclase ratio of the fractionating phases was high and accordingly Sc decrease with CaO (not shown). Early Palaoco lavas and cones show decreasing Sr with increasing Ce indicating that fractionation of plagioclase in these magmas played a more dominant role. All Palaoco lavas and cones show plagioclase-rich phenocryst assemblages (20–50% plagioclase phenocrysts) and this difference between petrography and chemistry suggests that the observed plagioclase-rich phenocryst assemblage crystallized at shallow levels (lower pressure) but did not fractionate. This probably reflects that fractionation, except for the early Palaoco lavas, occurred in magma chambers less shallow than those the magmas erupted from.

It is unlikely that the geochemical variations observed within the Fortunoso OIB-group lavas result from fractional crystallization of a uniform parental magma composition. Nb and K have similar compatibilities in basaltic magma and their ratio is therefore not expected to vary as basalt differentiates to basaltic andesites. However, a strong

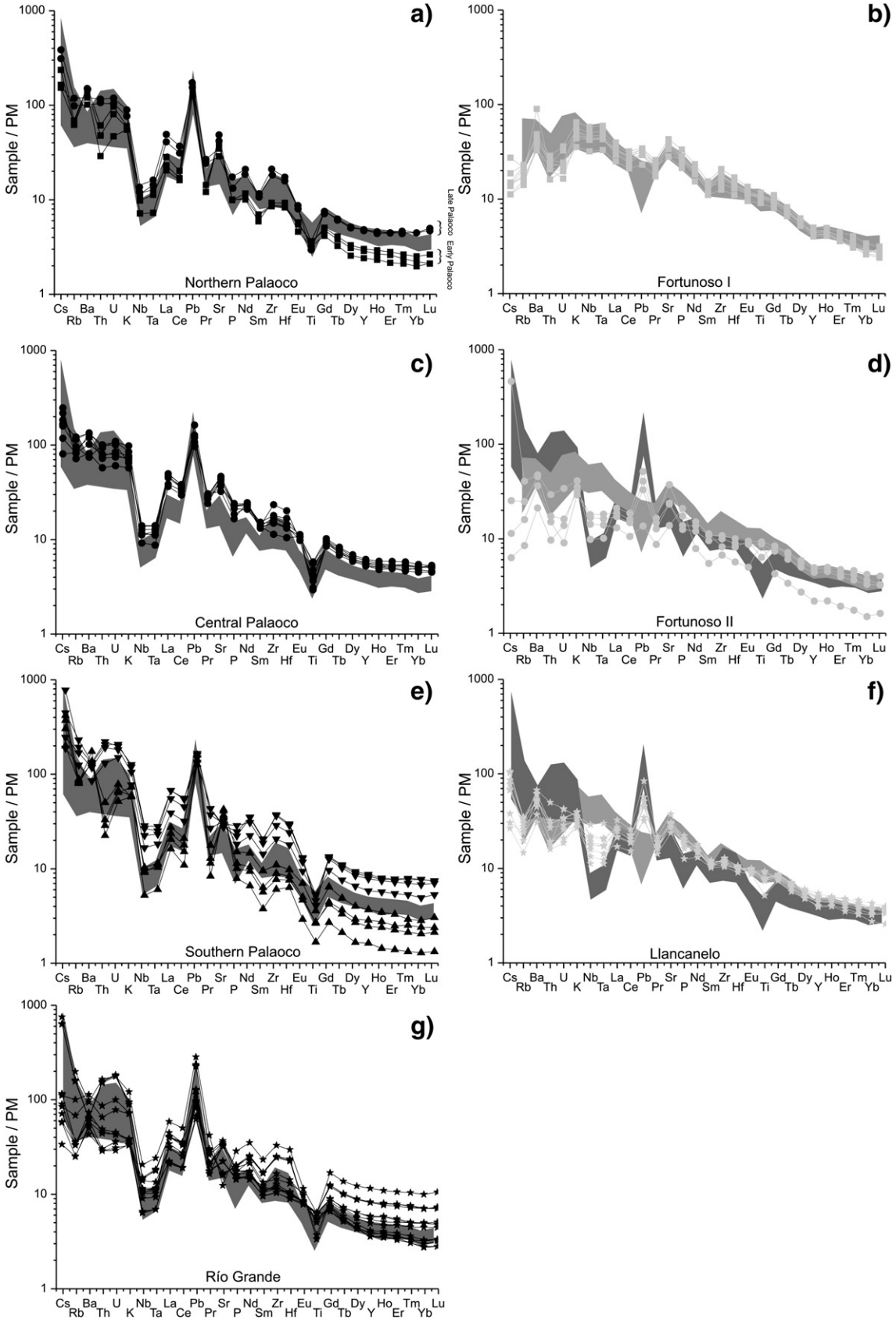

Fig. 7. Primitive mantle normalized incompatible element patterns. Laguna del Maule (indicated by a dark shadow) and Río Colorado (light shadow) are shown for comparison. Note the high abundance of incompatible elements in the upper part of the Northern Palaoco, Central Palaoco profiles and the Southern Group II in contrast to lower abundances the lower part of the Northern Palaoco profile and Southern Group I. Fortunoso I resembles Río Colorado and Fortunoso II shows large variation in incompatible element abundances all intermediate between Laguna del Maule and Río Colorado. Río Grande lavas show a stronger arc signature than Llancanelo. Primitive mantle normalizing values from Sun and McDonough (1989), Río Colorado from Søager and Holm (in preparation) and Laguna del Maule from Holm et al. (in preparation).

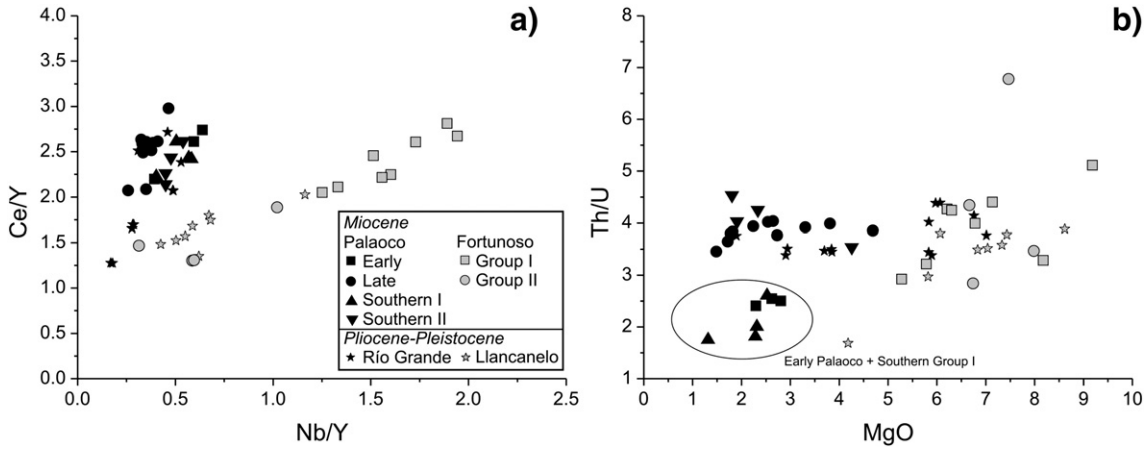

Fig. 8. a) The alkaline Fortunoso and Llancanelo cones and lavas correlate, ranging to high Nb/Y at low Ce/Y values in contrast to the arc-like Palaoco lavas and b) the anomalously low Th/U ratios in Early Palaoco and Southern Group I distinguish them from other Palaoco lavas.

decrease in $(Nb/K)_N$ with decreasing MgO is observed (not shown) in Fortunoso I lavas. Also the isotopic ratios of Sr, Nd and Pb should not vary in a suite of lavas produced by fractional crystallization of uniform parental magma, however large variation in Pb-isotopic compositions is observed within both Fortunoso Groups (Fig. 11). The systematic variations of both isotope and incompatible element ratios with very similar partition coefficients cannot be explained by differences in the degree of partial melting or by fractional crystallization but must instead reflect mixing between different components from a heterogeneous mantle source (or crustal assimilation, see Section 7.2). Constant Al_2O_3/CaO ratios indicate a lower clinopyroxene/plagioclase ratio in the fractionated mineral assemblage than observed in the Palaoco Groups.

7.2. Crustal contamination vs. subduction related fluids

7.2.1. Palaoco and Río Grande

Lavas influenced by subduction related fluids are expected to be low in Nb and Ta and rich in Pb, Sr, Ba and alkalis (e.g. Zanetti et al., 1999). The Payenia as well as Patagonian back-arc mantle sources record an eastward decrease of slab components, e.g. Ba, U and Pb (Stern et al., 1990; Gorring and Kay, 2001; Rivalenti et al., 2004). A probable source for enrichment of U, Th, alkali and alkaline earth elements compared to REE and HFSE is the subducted oceanic crust (Hickey et al., 1986). High Th/Ta and Ba/Nb in Palaoco and Río Grande lavas may similarly be explained as the result of high influence of elements supplied by the Nazca Plate (Fig. 12). As these ratios decrease with time, it seems that this influence decreases with time from Early Palaoco, through Late Palaoco to Río Grande lavas. Rocks from Late Palaoco and Río Grande show La/Nb and Ba/Nb ratios similar to basalts erupted in Laguna del Maule. Additionally, the normalized patterns of the Late Palaoco and Río Grande exhibit negative anomalies of Nb and Ta with respect to Ce and Th, and an enrichment of LILEs normally interpreted as characteristic features of volcanic arc rocks (Fig. 7) (e.g. Stern et al., 1990).

Sr isotope ratios do not show clear signs of contamination by upper continental crust (would result in higher $^{87}Sr/^{86}Sr$ ratios, unless the crust was very young). The isotopic similarity of Late Palaoco rocks to the volcanic arc leads us to conclude that a source enrichment similar to that of the arc basalts is responsible for the geochemical character

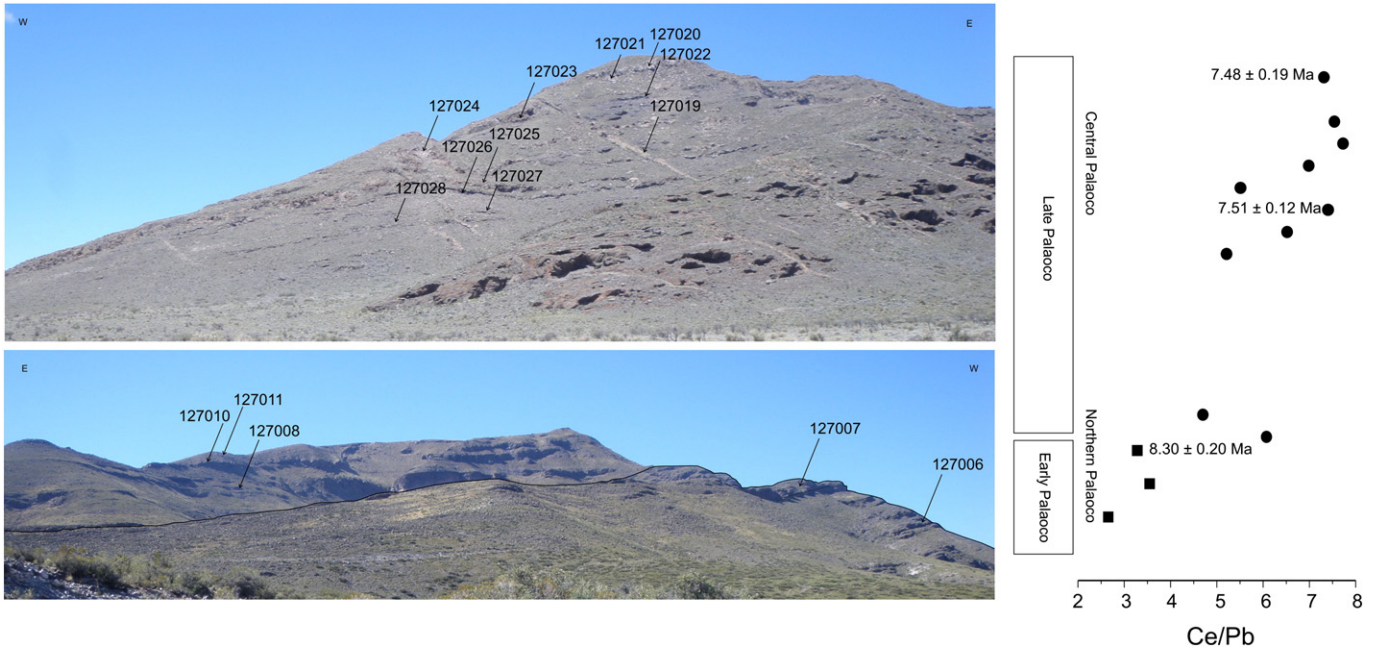

Fig. 9. Photographs showing the location of sampled lava flows in the Northern (lower photo) and Central Palaoco profile (upper photo) and the geochemical evolution from Early to Late Palaoco. We treat the upper lavas of the Northern profile along with the Central profile, i.e. Late Palaoco, on the basis of geochemical similarities, e.g. similar Ce/Pb.

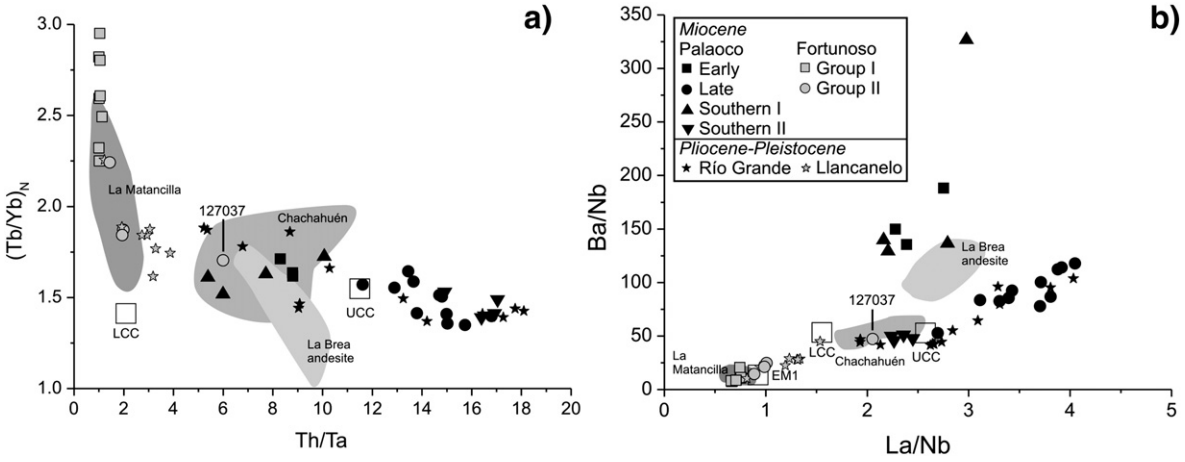

Fig. 10. a) $(Tb/Yb)_N$ vs. Th/Ta showing the intermediate nature of sample 127037 (normalization after Sun and McDonough, 1989) and b) Ba/Nb vs. La/Nb also highlighting the incompatible trace element similarities between sample 127037 and the Southern Palaoco II lavas. Note also the anomalously high Ba/Nb ratios in Early Palaoco lavas. Lower Continental Crust (LCC) and Upper Crustal Crust (UCC) are from Rudnick and Gao (2003). La Brea andesites (Nullo et al., 2002), Chachahuén (Kay et al., 2006b), Matancilla (Dyhr et al., 2013).

observed in Late Palaoco, that is to say by subduction-related fluids, not crustal assimilation.

The same features are evident in Early Palaoco rocks, which are extremely enriched fluid mobile elements relative to other incompatible elements, e.g. resulting in very low Th/U ratios. The La Brea andesites have high Ba/Nb (80–130) and Ba/La ratios that resemble Early Palaoco and Southern Group I. These relative Ba-enrichments are higher than seen in the present day SVZ (Southern Volcanic Zone). Early Palaoco lavas also deviate from the main Late Palaoco trend towards high Ba/Th (>200). Early Palaoco lavas have intermediate La/Nb of 2–3 (Fig. 10) and high Ba/Nb (125–325) (Fig. 10). Such trace element characteristics are similar to high grade feldspar-bearing depleted lower crust (LCC, Rudnick and Gao, 2003) implying that lower crustal contamination might affect the geochemical signature of Early Palaoco magmas. The Ce/Pb ratio indicated for the contaminant (<5) (Fig. 13a) is similar to the average LCC of Rudnick and Gao (2003). We test this hypothesis by mixing a possibly uncontaminated Late Palaoco sample (127025) and LCC (Fig. 13b) (details are in figure caption). Nb/U and La/Nb (Fig. 11) reflect the mantle source or addition of material to the magmas, because these ratios are not fractionated noticeably by melting or fractional crystallization. Our model suggests incorporation of up to 80% bulk LCC in the magmas which seems unreasonably high. The

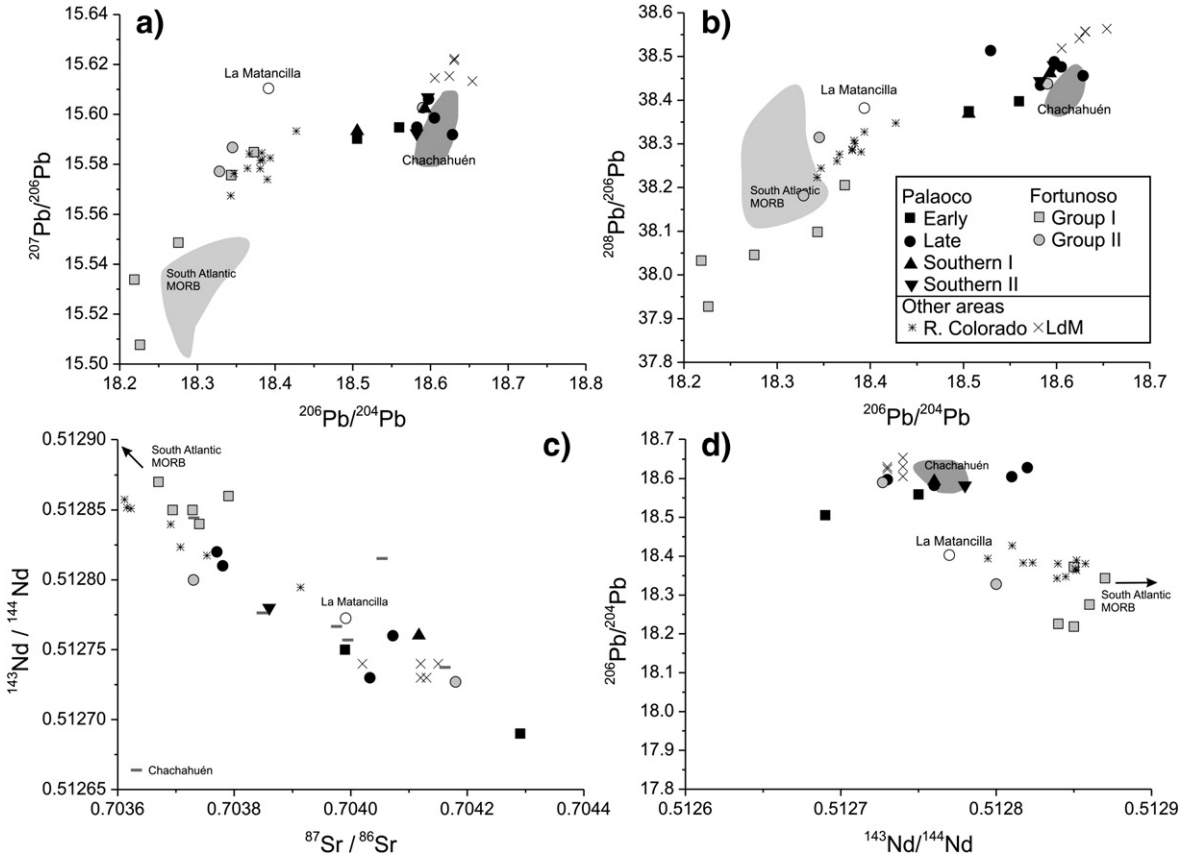

Fig. 11. Isotopic composition of Sr, Nd and Pb from Palaoco and Fortunoso. Also plotted are Laguna del Maule (LdM) (Holm et al., in preparation), Chachahuén (Kay et al., 2006b) and Río Colorado (R. Colorado) (Søager and Holm, in preparation). See text for details.

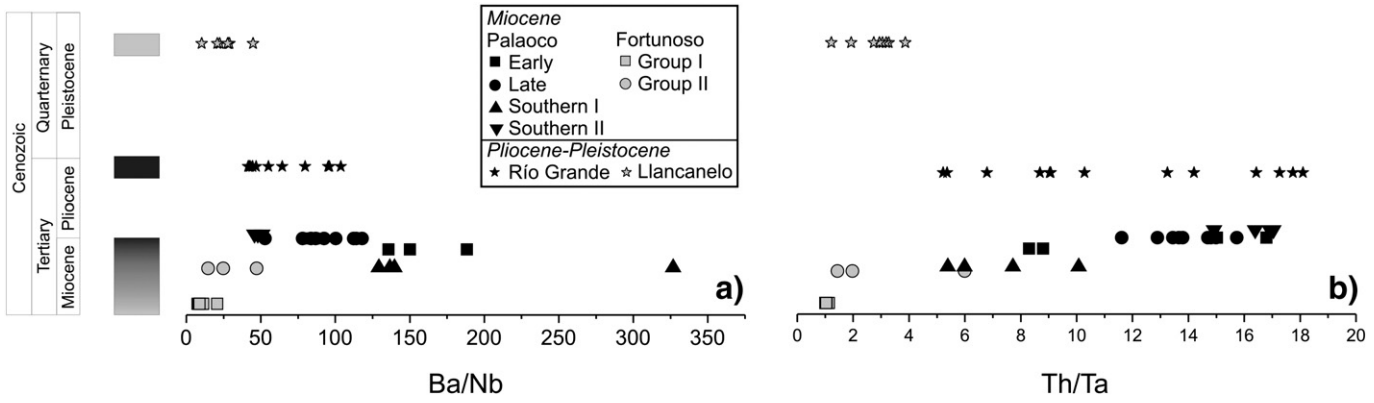

Fig. 12. The variation of Ba/Nb and Th/Ta through time. Note the dramatic increase in Ba/Nb in Early Palaoco rocks and Southern Group I rocks and the high Th/Ta for Late Palaoco and Southern Group II. See text for discussion.

modeled percentages are uncertain as the composition of the local assimilating melt is unknown. The amount of assimilation would be overestimated if the assimilated material was small degree melts of the crust with higher contents of crust incompatible elements than the bulk rocks. In contrast, if LCC was added to the source mantle instead of a Palaoco magma, a much smaller percentage of crust would be needed to explain the variation. It is possible that this component of lower crust was derived by subduction erosion (e.g. Kay and Kay, 1993; Stern, 2011). The crust may have melted and mixed with asthenospheric mantle melts after transportation to the back-arc mantle by the slab and mantle flow. Such processes are not easily distinguished from local crustal contamination, but the high contribution from slab fluids or melts (e.g. high Ba and U, resulting in low Nb/U and extremely high Ba/Nb (Fig. 10)) in Early Palaoco lavas seems to favor addition of subduction related fluids to the Palaoco mantle source over crustal contamination.

7.2.2. Fortunoso

Incompatible trace element ratios (e.g. La/Yb (10–20), Ba/La (10–15), Ba/Nb (6–10) and Cs/Rb (0.008–0.012)) of the Fortunoso rocks are close to or in the range of intraplate basalts (La/Yb (~17), Ba/La (~9), Ba/Nb (~6) and Cs/Rb (~0.0075) Willbold and Stracke, 2006). From the low $^{87}Sr/^{86}Sr$ ratios and the relatively high MgO (10–5 wt.%) it is unlikely that upper crustal assimilation played a major role in changing the composition of the basaltic magmas. However, the enhanced Th/Ta in Fortunoso II and anomalously high ratio in sample 127037 (~6) may indicate an increasing proportion of sediment-induced enrichment from Fortunoso I to II and especially for sample 127037 (Fig. 10a) (Hole et al., 1984). Lower crustal contamination has been inferred for some Nevado lavas (Søager and Holm, in preparation), and may also play an important role in the generation of the geochemical signature in Fortunoso I and Llancanelo rocks. Relatively high Ba/Th (100–200), low Ce/Pb and low Nb/U (Fig. 13) points toward contamination of the original EM-1 like source by lower crust.

7.3. Depth of melting

Low $(Tb/Yb)_N$ (1.30–1.75)) indicate a shallow origin for the Palaoco magmas and a negative correlation with Th/Ta indicate decreasing depths of melting as the subduction zone input increases. $(Tb/Yb)_N$ ratios and REE patterns indicate deeper melting of Fortunoso magmas than Palaoco and Río Grande magmas. Shown for comparison are Chachahuén and La Brea lavas both displaying $(Tb/Yb)_N$ ratios similar to Palaoco and lower than Fortunoso, with Chachahuén ranging 1.4–2.0 and La Brea slightly lower ranging 1.0–1.8.

Rocks of Southern Palaoco I and Río Grande are transitional between Late Palaoco and Fortunoso I in character with respect to incompatible trace element ratios. The influences of elements supplied by the subducting plate are less dominant than in Early Palaoco. The Fortunoso Group I show the higher $(Tb/Yb)_N$ (2.24–2.99) interpreted to be the result of partial melting in the garnet stability field.

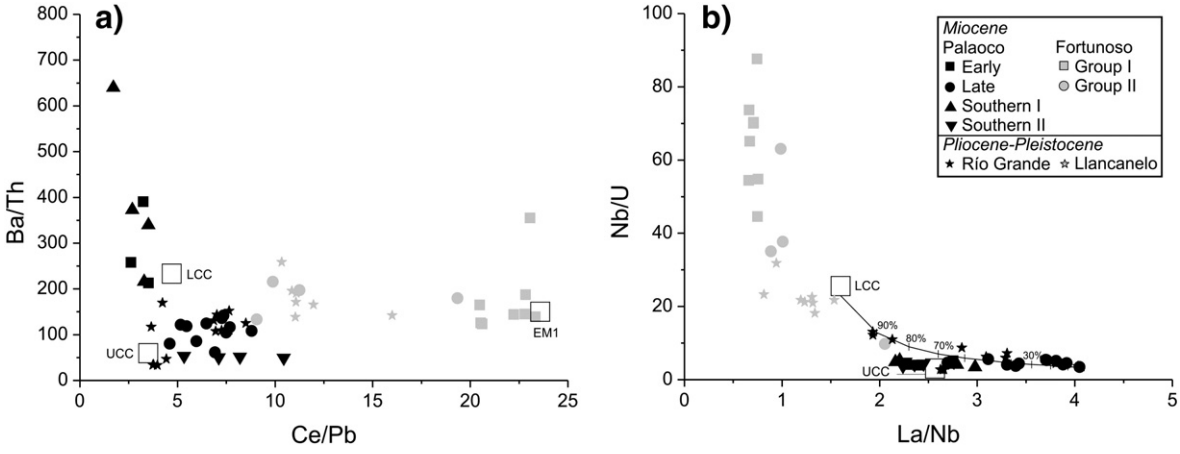

Fig. 13. a) Ba/Th vs. Ce/Pb showing the OIB-like character of Fortunoso Group I. Lower Continental Crust (LCC) and Upper Continental Crust (UCC) both have much lower Ba/Th than Early Palaoco. B) Nb/U vs. La/Nb showing mixing between LCC and sample 127025. Parameters used in the calculation are: LCC: Nb = 5 ppm, U = 0.2 ppm and La = 8 ppm and uncontaminated sample 127025: Nb = 7.8 ppm, U = 2.3 ppm and La = 31.9 ppm. LCC and UCC are from Rudnick and Gao (2003) and EM1 is from Zindler and Hart (1986).

7.4. Evolution and origin of Fortunoso and Palaoco volcanic areas

Chemical and isotopic data show that the magmas that erupted during the Early Miocene (Fortunoso I) were dominated by an intraplate-like chemical signature. The Fortunoso I mantle source is apparently an asthenospheric mantle component with a trace element composition different from normal MORB asthenosphere. Higher Ba/Nb (~10) than in N-MORB (Sun and McDonough, 1989) might reflect an addition of slab components, however the Fortunoso I lavas have higher U/Pb (0.2–0.3) and lower La/Nb (~0.7) than N-MORB (0.16 and 1.1 respectively Sun and McDonough, 1989) in contrast to what would be expected of fluid addition or melts from subducted material. The Fortunoso I end-member is geochemically very similar to the EM-1 like Río Colorado end-member for Pleistocene–Holocene Payenia described by Søager and Holm (in preparation). However, the small positive Pb anomalies in some samples, which are in contrast to the more recent Río Colorado OIB-like end-member, signals a small contribution from subduction components or crustal contaminants. The similarity between Early Miocene Fortunoso basalts, La Matancilla and recent Río Colorado basalts show the long-lived nature of an OIB-type component in the back-arc mantle. Although no additional geochemical data have yet been presented, the Early Miocene Cerrillos Formation may in general be characterized by OIB-type magmas similar to Fortunoso I. Silvestro et al. (2009) mapped the Cerrillos lavas both at the western slopes of Sierra de Palaoco and further north in Sierra de la Ventana south of Malargüe. This volcanism has been proposed to be related to extensional tectonics at the end of a period lasting from the Oligocene when the South American plate decellerated (Silver et al., 1998).

Isotopically, Fortunoso I range from compositions much like Early Miocene Matancilla (Dyhr et al., 2013) and Pleisotocene Río Colorado (Søager and Holm, in preparation) to compositions not unlike South Atlantic N-MORB. A few samples have even more unradiogenic Pb than the latter (Fig. 11). This trend suggests that two OIB-type components can explain the mantle sources for Fortunoso I by variable relative contributions. The already described geochemical variation among the Late Miocene Fortunoso II samples that trend from OIB-type to arc-type is also displayed by the two samples analyzed for isotopic composition. At Huantraico (near Matancilla) the back-arc mantle became increasingly affected by subduction zone fluids already in the Early Miocene, as evidenced by a compositional transition with increasing slab influence upsection through the Huantraico plateau at 18–17 Ma (Dyhr et al., 2013). Recent investigations of volcanic rocks in the area west of Palaoco-Fortunoso, at Charilehue, Cordón del Burrero as well as at Cordon de Molle and other locations with activity in the Charilehue and Huincan I periods show that materials derived from the subduction channel influenced the mantle sources at 17–14 Ma (Nullo et al., 2002; Sruoga et al., 2008; Spagnuolo et al., 2012). Nevertheless, the transition displayed at Fortunoso II just prior to the Palaoco volcanism, indicates that the OIB-type mantle under Sierra de Palaoco still contributed somewhat to magmas in the Late Miocene, at 8.6 ± 0.2 Ma.

The very strong relative LILE enrichment in early Palaoco volcanism at 8.3 ± 0.2 Ma (and Southern I) most definitely is evidence for fluid metasomatism of its mantle source and we suggest that from this time onwards a subducting slab was positioned approximately 100 km below Palaoco as well as below La Brea further to the north. Subsequently, after a quiescence of ~1 Ma, the magmas erupted at Palaoco at 7.5 ± 0.1 Ma had acquired a different style of enrichment with Ba/La, Ba/Nb (Ba/Ta) ratios more like what is usual in the Holocene arc of the SVZ, and this part of Palaoco volcanism, which may largely have been erupted in a app. 0.5 Ma, is probably the most representative of the large basaltic–andesitic eruptions of Palaoco. Compared to Late Palaoco, the slightly younger Chachahúen volcanism (7.3–4.9 Ma) has significantly less arc imprint. For instance La/Ta is lower (28–42) in mafic Chachahuén rocks than in Late Palaco (47–70) and is also lower than for most of the subsequently erupted Río Grande group (33–70), and approach the Llancanelo magmas (22–30). It is likely that no OIB-type mantle was present in the Palaoco area and northwards after 8.3 Ma, during Palaoco (8.3–7.5 Ma) and La Brea (until c. 7–6 Ma; Nullo et al., 2002) volcanism. By contrast, at Chachahuén the OIB component was important during the Late Miocene as evident from the rather low La/Ta. During the Plio-Pleistocene Río Grande volcanism (2.9–0.7 Ma), OIB-type mantle reappeared as source component for the back-arc magmas and this influence increased during the Late Pleistocene Llancanelo volcanism.

The OIB-type magmas of Fortunoso and Matancilla must have had higher temperatures as they were extracted at depths in mantle where garnet was residual. The solidi of the likely fluid-enriched mantle sources of the arc-type magmas must have been lowered, and yet they did not melt in the garnet stability field but more shallowly. This was probably due to either mantle metasomatism in the wedge above the garnet stability field or a relatively cold mantle wedge. This seems also to be indicated by the relatively low Tb/Yb of mafic Chachahuén rocks.

Spagnuolo et al. (2012) coupled the eruption of the Charilehue Formation (18–14.5 Ma) with the acceleration after late Oligocene of the South American plate from a very low absolute speed to a westward movement resulting in compression and slab shallowing of the subducting Nazca plate and the development of a volcanic arc further east. The Charilehue volcanic rocks have a very weak arc-type enrichment, mostly with e.g. Ba/Nb < 30 and La/Nb < 1.5, which was suggested by Spagnuolo et al. (2012) to mark an initial arc development. In the present retro-arc area further to the north, in Cordón del Burrero, concomitant volcanism had a variable but up to much stronger arc signature, e.g. with mainly La/Nb ranging 1.5–3.5 but Ba/La relatively low: 14–20, and also for this northern complex initial arc volcanism was suggested (Sruoga et al., 2008). Subsequently in the Huincán I period (10–15 Ma) arc volcanism occurred both N of Palaoco near the rivers Salado and Atuel (around 35°S) (Nullo et al., 2002) and 50–100 km E of Palaoco on the San Rafael basement block (Litvak et al., 2008). The Huincán rocks of Nullo et al. (2002) have a geochemical signature (La/Nb = 2–3, Ba/Nb = 35–60) more like typical arc than Charilehue but less than at Palaoco, whereas those of El Zaino and other nearby volcanoes appears to have slightly less LREE- and Ba-enrichment and appear more akin to Chachahuén (Kay et al., 2006a; Litvak et al., 2008, 2010). The mantle source for these could not have been as that of the present day adjacent SVZ.

The Palaoco volcanism occurred at the end of, and subsequent to, the development over 10.5–8 Ma of the Malargüe fold and thrust belt (Silvestro et al., 2005; Giambiagi et al., 2008). We suggest that at this time a fully developed arc was present at around 69.5°W from Sierra de Palaoco to La Brea (app. 34.5–36.5°S). Activity in Sierra de Palaoco took place in two periods around 8.3 and 7.5 Ma, respectively, and according to the Ar analyses of Nullo et al. (2002) the La Brea activity lasted at least 4 Ma from 11 to 7 Ma. Volcanism with an unusually strong Ba- and Sr-enrichment in Early Palaoco and La Brea changed to volcanism that is similar to many Transitional SVZ magmas with e.g. La/Nb > 3 and Ba/La = 20–30. Miocene rocks with enrichment comparable to Late Palaoco is found only in some Cura Mallín, Trapa Trapa (Fig. 1) and Picchi Neuquen samples W of Cordillera del Viento (Kay et al., 2006a). In a considerable period onwards from the same time (8.3–3.5 Ma) Cerro Plateado and other volcanoes situated in the far back arc erupted magmas with an arc imprint stronger than for Charilehue (Litvak et al., 2010). It is possible that frontal arc volcanism translated from Palaoco–La Brea to the east in the Late Miocene and Early Pliocene.

There was a break in volcanism after emplacement of the Palaoco sequence (8.5–7.5 Ma) and before the eruption of geochemically similar lavas belonging to the Río Grande group at ~3 Ma Also, a dramatic change in eruption style occurred from the vast lava flows constituting the Palaoco plateau to the volumetrically minor basaltic volcanism of Río Grande. We regard the Río Grande lavas as back-arc volcanism caused by the release of fluids or melts from a subducting slab that was retreating towards the west following a period of flat slab

subduction under Palaoco latitudes. In this scenario, then, the east-dipping front of a flat slab migrates eastwards passing Palaoco around 8.3–7.5 Ma and on to Plateado where it appears to cause arc-volcanism for several Ma until, in the Early Pliocene it rolls back causing the weaker Río Grande volcanism at 3 Ma. The Llancanelo lavas erupted in the Palaoco Valley after ~0.7 Ma (Gudnason et al., 2012; Dyhr et al., 2013) were almost devoid of subduction zone components. The alkaline volcanism was initiated in the Nevado volcanic field ~130 km E of Río Grande at around 3 Ma (Gudnason et al., 2012; Søager et al., 2013), and had a temporal transition towards more OIB-like compositions as described by Saal (1994a). This development correlates well with the sketched scenario, because as the dipping slab rolls back resumption of intra-plate volcanism expanded westwards. The details of the Pleistocene–Holocene Payenia back-arc volcanism was recently discussed in detail by Gudnason et al. (2012) and Søager et al. (2013).

In summary, most of the Miocene volcanic rocks erupted after 20 Ma in the present retroarc and back-arc areas have been suggested to possess only a moderate contribution from subduction derived materials (e.g. Nullo et al., 2002; Litvak et al., 2008; Sruoga et al., 2008; Litvak et al., 2009; Silvestro et al., 2009; Spagnuolo et al., 2012). However, the Palaoco magmas were derived from mantle sources clearly enriched similarly as sources for Holocene SVZ magmas and was probably devoid of mantle components that, by contrast, characterized the Early Miocene OIB magmas of Fortunoso–Matancilla.

8. Conclusion

Volcanism of Sierra de Palaoco, southern Mendoza, is divided into (1) the Early Miocene Fortunoso I monogenetic eruptions of trachybasalts and alkali basalts, 20.8 ± 0.2 (2σ) Ma by ^{40}Ar–^{39}Ar, (2) the Late Miocene Fortunoso II basalts, also by monogenetic eruptions, 8.6 ± 0.2 Ma, (3) Early Palaoco andesites of the lower part of the voluminous lava succession, 8.3 ± 0.1 Ma, and (4) the Late Palaoco trachybasalts and more evolved lavas of the main part of the Palaoco succession which may have been erupted within a few hundred ka around 7.5 Ma. Later volcanic rocks of the area encompass the Plio-Pleistocene (2.87 ± 0.052 and 0.7 ± 0.2 Ma) Río Grande group of basalts-basaltic andesites and trachyandesites, and Late Pleistocene alkali basalts belonging to the Llancanelo Volcanic Field. Fractional crystallization explain the derivation of evolved rocks of each group, that took place without significant accompanying crustal contamination, as inferred from constant incompatible element and isotopic ratios during magmatic evolution. With some notable exceptions, the geochemical character of the rocks were generated during mantle melting.

Fortunoso I show typical OIB-type trace element patterns, whereas Fortunoso II display a transition to arc-type patterns. Early Palaoco rocks have strong relative enrichment in Ba, Sr, Pb and U, which is ascribed to an unusually enhanced role for fluid-enrichment in the source, e.g. Ba/La around 60. Late Paloco rocks have incompatible element enrichment very like Holocene arc magmas. HREE fractionation is considerable for Fortunoso I ($Tb/Yb_{cho} = -2.24$–2.99) and were derived from a garnet-bearing mantle. $Tb/Yb_{cho} = -1.30$–1.75 in the Palaoco succession signals shallow melt extraction.

Isotopically Fortunoso I shows variation between two EM1-type mantle components and overlaps with other OIB-type Miocene and Pleistocene rocks from Payenia. This indicates the episodic presence over >20 Ma of the same enriched mantle source composition. The Palaoco rocks have distinctly different isotopic compositions with more radiogenic Pb and Sr and less radiogenic Nd similar to typical Holocene magmas of the Andes Transitional Southern Volcanic Zone.

Middle–Late Miocene magmatism in the present back-arc area show only incipient subduction zone source enrichment. The exception is the Palaoco and La Brea (to the north) volcanism which show full typical arc-enrichment, and thereby indicate that at 8.3–7.5 Ma a frontal arc was established. The succession of volcanic events and magma types, as well as quiescence in the Palaoco area and in the far back-arc to the east, are suggested to reflect eastward extension of a flat slab. The existing geochronological and geochemical data further support a scenario where the dipping part of the slab east of the flat slab area translated 50 km from Palaoco to the east before the Late Pliocene, and subsequently retreated causing renewed arc-volcanism in the Río Grande area and alkaline volcanism in the Nevado Volcanic field to the east, and, with further retreat to west, the alkaline volcanism moved to the Palaoco area in the Late Pleistocene.

Supplementary data to this article can be found online at http://dx.doi.org/10.1016/j.jvolgeores.2013.08.005.

Acknowledgements

Simon Normann Lauritzen and Jesper Holst are thanked for their assistance during field work. Laurence Page, Toni Larsen and Toby Leeper are thanked for analytical assistance and we thank Jørgen Kystol for excellent major and trace element analyses. Nina Søager is thanked for many fruitful discussions. Two anonymous reviewers are thanked for their comments that greatly strengthened the paper. We greatly acknowledge the support to PMH from the Danish Research Council, grant 272-07-0514 and the Faculty of Science for a PhD stipend to CTD.

References

Bermúdez, A., Delpino, D., Frey, F., Saal, A., 1993. Los basaltos de retroarco extraandinos. In: Ramos, V.A. (Ed.), Geología y Recursos Naturales de Mendoza, Relatorio. XII Congreso Geológico Argentino y II Congreso de Exploración de Hidrocarburos, Mendoza, pp. 161–173.

Bertotto, G.W., Cingolani, C.A., Bjerg, E.A., 2009. Geochemical variations in Cenozoic back-arc basalts at the border of La Pampa and Mendoza provinces, Argentina. J. S. Am. Earth Sci. 28, 360–373.

Combina, A., Nullo, F., 2000. La Formación Loma Fiera (Mioceno superior) y su relación con el volcanismo y el tectonismo neógeno, Mendoza. Rev. Asoc. Geol. Argent. 55, 201–210.

Dalrymple, G.B., Lanphere, M.A., 1971. $^{40}Ar/^{39}Ar$ technique of K-Ar dating: a comparison with the conventional technique. Earth Planet. Sci. Lett. 12, 300–308.

Dessanti, R., 1973. Descripción geológica de la hoja 29d, Bardas Blancas. Provincia de Mendoza. Carta Geológica de la República Argentina, escala 1:200.000, Servicio Geológico Nacional, 70 pp., Buenos Aires.

Dyhr, C.T., Holm, P.M., Llambías, E.J., Scherstén, A., 2013. Subduction controls on Miocene back-arc lavas from Sierra de Huantraico and La Matancilla and new $^{40}Ar/^{39}Ar$ dating from the Mendoza Region, Argentina. Lithos 178, 67–83.

Folguera, A., Ramos, V.A., 2011. Repeated eastwards shifts of arc magmatism in the Southern Andes: a revision of the long-term pattern of Andean uplift and magmatism. J. S. Am. Earth Sci. 32, 531–546.

Folguera, A., Naranjo, J.A., Orihashi, Y., Sumino, H., Nagao, K., 2009. Retroarc volcanism in the northern San Rafael Block (34°–35°30′S), southern Central Andes: occurrence, age and tectonic setting. J. Volcanol. Geotherm. Res. 186, 169–185.

Folguera, A., Orts, D., Spagnuolo, M., Rojas Vera, E., Litvak, V., Sagripanti, L., Ramos, M.E., Ramos, V.A., 2011. A review of Late Cretaceous to Quaternary palaeogeography of the southern Andes. Biol. J. Linn. Soc. 2011 (103), 250–268.

Frey, F.A., Gerlach, D.C., Hickey, R.L., Lopez-Escobar, L., Munizaga-Villavicencio, F., 1984. Petrogenesis of the Laguna del Maule volcanic complex, Chile (36°S). Contrib. Mineral. Petrol. 88, 133–149.

Galland, O., Hallot, E., Cobbold, P.R., Buffet, G., 2007. Volcanism in a compressional Andean setting: a structural and geochronological study of Tromen volcano (Neuquén province, Argentina). Tectonics 26, 1–24.

Giambiagi, L., Bechis, F., García, V., Clark, A.H., 2008. Temporal and spatial relationships of thick- and thin-skinned deformation: a case study from the Malargüe fold-and-thrust belt, southern Central Andes. Tectonophysics 459, 123–139.

Gorring, M.L., Kay, S.M., 2001. Mantle processes and sources of Neogene slab window magmas from southern Patagonia, Argentina. J. Petrol. 42, 1067–1094.

Groeber, P., 1946. Observaciones geológicas a lo largo del meridiano 70. 1 Hoja Chos Malal. Rev. Soc. Geol. Argent. 1, 177–208.

Gudnason, J., Holm, P.M., Søager, N., Llambías, E.J., 2012. Geochronology of the late Pliocene to recent volcanic activity in the Payenia back-arc volcanic province, Mendoza Argentina. J. S. Am. Earth Sci. 37, 191–201.

Hernando, I.R., Llambías, E.J., González, P.D., Sato, K., 2012. Volcanic stratigraphy and evidence of magma mixing in the Quarternary Payún Matrú volcano, Andean back-arc in western Argentina. Andean Geol. 39, 158–179.

Hickey, R.L., Frey, F.A., Gerlach, D.C., 1986. Multiple sources for basaltic arc rocks from the southern volcanic zone of the Andes (34°S–41°S): trace element and isotopic evidence for contributions from subducted oceanic crust, mantle and continental crust. J. Geophys. Res. 91, 5963–5983.

Hole, M.J., Saunders, A.D., Marriner, G.F., Tarney, J., 1984. Subduction of pelagic sediments: implications for the origin of Ce-anomalous basalts from the Mariana Islands. J. Geol. Soc. 141, 453–472.

Holm, P.M., Søager, N., Dyhr, C.T., 2013n. The role of crust and fluids in the generation of arc magmas in the SVZ of the Andes (in preparation).

Inbar, M., Risso, C., 2001. A morphological and morphometric analysis of a high density cinder cone volcanic field — Payún Matrú, south-central Andes, Argentina. Z. Geomorphol. 45, 321–343.
Kay, S.M., Copeland, P., 2006. Early to middle back-arc magmas of the Neuquén Basin: Geochemical consequences of slab shallowing and the westward drift of South America. Evolution of an Andean margin: a tectonic and magmatic view from the Andes to the Neuquén Basin (35°–39° S lat). Geol. Soc. Am. Spec. Pap. 407, 185–214.
Kay, R.W., Kay, S.M., 1993. Delamination and delamination magmatism. Tectonophysics 219, 177–189.
Kay, S.M., Orrell, S., Abbruzzi, J.M., 1996. Zircon and whole rock Nd–Pb isotopic evidence for a Grenville age and a Laurentian origin for the Precordillera terrane in Argentina. J. Geol. 104, 637–648.
Kay, S.M., Gorring, M.L., Ramos, V.A., 2004. Magmatic sources, setting and causes of Eocene to Recent Patagonian plateau magmatism (36°S to 52°S latitude). Rev. Asoc. Geol. Argent. 59, 556–568.
Kay, S.M., Burns, W.M., Copeland, P., Mancilla, O., 2006a. Upper Cretaceous to Holocene magmatism and evidence for transient Miocene shallowing of the Andean subduction zone under the northern Neuquén Basin. Evolution of an Andean margin: a tectonic and magmatic view from the Andes to the Neuquén Basin (35°–39° S lat). Geol. Soc. Am. Spec. Pap. 407, 19–60.
Kay, S.M., Mancilla, O., Copeland, P., 2006b. Evolution of the late Miocene Chachahuén volcanic complex at 37°S over a transient shallow subduction zone under the Neuquén Andes. Evolution of an Andean margin: a tectonic and magmatic view from the Andes to the Neuquén Basin (35°–39° S lat). Geol. Soc. Am. Spec. Pap. 407, 215–246.
Kystol, J., Larsen, L.M., 1999. Analytical procedures in the rock geochemical laboratory of the Geological Survey of Denmark and Greenland. Geol. Greenl. Surv. Bull. 184, 59–62.
Le Maitre, R.W. (Ed.), 2002. Igneous Rocks, A Classification and Glossary of Terms, 2nd edition. Cambridge University Press, Cambridge.
Litvak, V., Folguera, A., Ramos, V.A., 2008. Determination of an arc-related signature in Late Miocene volcanism over the San Rafael Block, Southern Central Andres (34°30-37°), Argentina: the Payenia shallow subduction zone. 7th International Symposium on Andean Geodynamics, Niza, Extended Abstracts, pp. 289–291.
Litvak, V., Folguera, A., Ramos, V.A., 2009. La expansión hacia el antepaís del arco volcánico mioceno al sur de la provincia de Mendoza, Andes Centrales del Sur. XII Congreso Geológico Chileno. Electronic Files, Santiago, Chile.
Litvak, V., Spagnuolo, M.G., Folguera, A., Ramos, V.A., 2010. Evolution of Middle to Late Miocene arc-related magmatism between 35° and 38°S, Southern Central Andes, Argentina. AGU Meeting of the Americas, Foz do Iguacu, Brazil.
Llambías, E.J., Bertotto, G.W., Risso, C., Hernando, I.R., 2010. El volcanismo cuaternario en el retroarco de Payenia: una revision. Rev. Asoc. Geol. Argent. 67, 278–300.
Nullo, F.E., Stephens, G.C., Otamendi, J., Baldauf, P.E., 2002. El volcanismo del Terciario superior del sur de Mendoza. Rev. Asoc. Geol. Argent. 57, 119–132.
Oncken, O., Hindle, D., Kley, J., Elger, K., Victor, P., Schemmann, K., 2006. Deformation of the central Andean upper plate system, Facts, Fiction, and constraints for plateau models. In: Oncken, et al. (Ed.), The Andes Active Subduction Orogeny. Frontiers in Earth Sciences, vol. 1. Springer, Berlin Heidelberg, pp. 1–27.
Ramos, V.A., 1978. Estructura. In: Rolleri, E.O. (Ed.), Geología y Recursos Naturales de la Provincia del Neuqúen. VII° Congreso Geológico Argentino (Neuqúen), Relatorio, pp. 99–118.
Ramos, V.A., Folguera, A., 2011. Payenia volcanic province in the Southern Andes: an appraisal of an exceptional Quaternary tectonic setting. J. Volcanol. Geotherm. Res. 201, 53–64.
Ramos, V.A., Kay, S.M., 2006. Overview over the tectonic evolution of the southern Central Andes of Mendoza and Neuquén (35°–39° S latitude. Evolution of an Andean margin: a tectonic and magmatic view from the Andes to the Neuquén Basin (35°–39° S lat). Geol. Soc. Am. Spec. Pap. 407, 1–18.
Rivalenti, G., Mazzucchelli, M., Laurora, A., Ciuffi, S.I.A., Zanetti, A., Vannucci, R., Cingolani, C.A., 2004. The back-arc mantle lithosphere in Patagonia, South America. J. S. Am. Earth Sci. 17, 121–152.
Rudnick, R.L., Gao, S., 2003. Composition of the continental crust. Treatise on Geochemistry, 3.01, pp. 1–64.
Saal, A.E., 1994a. Petrology and Geochemistry of Intra-back Arc Basalts from the Argentine Andes. Department of Earth, Atmospheric and Planetary Sciences, Massachussetts Institute of Technology (174 pp.).
Saal, A., 1994b. Petrology and geochemistry of intra-back arc basalts from the Argentine Andes [M.S. thesis]: Cambridge. Massachusetts Institute of Technology, Massachusetts 164.
Silver, P.G., Russo, R.M., Lithgow-Bertelloni, C., 1998. Coupling of South American and African plate motion and plate deformation. Science 279, 60–63.
Silvestro, J., Kraemer, P., Achilli, F., Brinkworth, W., 2005. Evolución de las cuencas sinorogénicas de la Cordillera Principal entre 35°–36°S, Malargüe. Rev. Asoc. Geol. Argent. 60, 627–643.
Silvestro, J., Atencio, M., Silvestro, J., Atencio, M., 2009. La cuenca cenozoica del río Grande y Palauco: edad, evolución y control estructural, faja plegada de Malargüe (36°S). Rev. Asoc. Geol. Argent. 65, 154–169.
Søager, N., Holm, P.M., 2013n. Melt-peridotite reactions in upwelling EM1-type eclogite bodies: constraints from alkaline basalts in Payenia, Argentina. Chem. Geol. (in preparation).
Søager, N., Holm, P.M., Llambías, E.J., 2013. Payenia volcanic province, southern Mendoza, Argentina: OIB mantle upwelling in a backarc environment. Chem. Geol. 349–350, 36–53.
Spagnuolo, M.G., Folguera, A., Litvak, V., Rojas Vera, E.A., Ramos, V.A., 2012. Late Cretaceous arc rocks in the Andean retroarc region at 36.5°S: evidence supporting a Late Cretaceous slab shallowing. J. S. Am. Earth Sci. 38, 44–56.
Sruoga, P., Rubinstein, N.A., Etcheverría, M.P., Cegarra, M., Kay, S.M., Singer, B., Lee, J., 2008. Estadío inicial del arco volcánic neógeno en la Cordillera Principal de Mendoza (35°S). Rev. Asoc. Geol. Argent. 63, 454–469.
Stern, C.R., 2011. Subduction erosion: rates, mechanisms, and its role in arc magmatism and the evolution of the continental crust and mantle. Gondwana Res. 20, 284–308.
Stern, C.R., Frey, F.A., Futa, K., Zartman, R.E., Peng, Z., Kyser, K.T., 1990. Trace-element and Sr, Nd, Pb and O isotopic composition of Pliocene and Quarternary alkali basalts of the Patagonian Plateau lavas of southernmost South America. Contrib. Mineral. Petrol. 104, 294–308.
Sun, S.S., McDonough, W.F., 1989. Chemical and isotopic systematic of oceanic basalts: implications for mantle composition and processes. In: Saunders, A.D., Norry, M.J. (Eds.), Magmatism in the Ocean Basins. Geological Society of London, Special Publication, 42, pp. 313–345.
Willbold, M., Stracke, A., 2006. Trace element composition of mantle end-members: implications for recycling of oceanic and upper and lower continental crust. Geochem. Geophys. Geosyst. 7. http://dx.doi.org/10.1029/2005GC001005.
Zanetti, A., Mazzucchelli, M., Rivalenti, G., Vannucci, R., 1999. The Finero phlogopite–peridotite massif: an example of subduction-related metasomatism. Contrib. Mineral. Petrol. 134, 107–122.
Zindler, A., Hart, S., 1986. Chemical geodynamics. Ann. Rev. Earth Planet. Sci. Lett 14, 493–571.